RSC Advances

PAPER

View Article Online
View Journal | View Issue

Cite this: *RSC Adv.*, 2022, **12**, 23644

Design and synthesis of new bis(1,2,4-triazolo[3,4-*b*][1,3,4]thiadiazines) and bis((quinoxalin-2-yl)phenoxy)alkanes as anti-breast cancer agents through dual PARP-1 and EGFR targets inhibition†

Fatma M. Thabet,[a] Kamal M. Dawood,[*a] Eman A. Ragab,[a] Mohamed S. Nafie[b] and Ashraf A. Abbas[*a]

A number of new 1,ω-bis((acetylphenoxy)acetamide)alkanes **5a–f** were prepared then their bromination using NBS furnished the novel bis(2-bromoacetyl)phenoxy)acetamides **6a–f**. Reaction of **6a–f** with 4-amino-5-substituted-4*H*-1,2,4-triazole-3-thiol **7a–d** and with *o*-phenylenediamine derivatives **9a** and **b** afforded the corresponding bis(1,2,4-triazolo[3,4-*b*][1,3,4]thiadiazine) derivatives **8a–l** and bis(quinoxaline) derivatives **10a–e** in good yields. The cytotoxicity of the synthesized compounds as well as apoptosis induction through PARP-1 and EGFR as molecular targets was evaluated. Three compounds, **8d**, **8i** and **8l**, exhibited much better cytotoxic activities against MDA-MB-231 than the drug Erlotinib. Interestingly, compound **8i** induced apoptosis in MDA-MB-231 cells by 38-fold compared to the control arresting the cell cycle at the G2/M phase, and its treatment upregulated P53, Bax, caspase-3, caspase-8, and caspase-9 gene levels, while it downregulated the Bcl2 level. Compound **8i** exhibited promising dual enzyme inhibition of PARP-1 (IC_{50} = 1.37 nM) compared to Olaparib (IC_{50} = 1.49 nM), and EGFR (IC_{50} = 64.65 nM) compared to Erlotinib (IC_{50} = 80 nM). These results agreed with the molecular docking studies that highlighted the binding disposition of compound **8i** inside the PARP-1 and EGFR protein active sites. Hence, compound **8i** may serve as a potential anti-breast cancer agent.

Received 8th June 2022
Accepted 10th August 2022

DOI: 10.1039/d2ra03549a

rsc.li/rsc-advances

1. Introduction

Cancer is a serious public health issue that affects people all over the world. The statistics on incidence and mortality showed that it is increasing in both economically emerging and developed countries. Breast cancer is the most common malignancy in women, accounting for 23% of all cancer diagnoses and 14% of cancer deaths.[1] As a result, breast cancer cells have been found to be more reliant on DNA repair pathways than normal cells, making them more vulnerable to DNA-damage response suppression.[2] Anticancer research continues to be a priority, with more effective and selective chemotherapeutic anticancer drugs urgently needed.

The presence of a carboxamide functionality in the composition of organic molecules was found to be essential in many clinically approved synthetic and naturally derived drugs. The carbonyl and amine groups in the carboxamide function had an interesting attention where they act as a hydrogen-bond acceptor (HBA) and a hydrogen-bond donor (HBD), respectively.[3–6] It is well known that amide-based flexible pharmacophore had a significant role in enhancing the biological activity due to its hydrogen acceptor/donor (HAD) behaviour.[3] A number of 1,2,4-triazole-based fused heterocycles had received a wide range of medicinal applications as appeared in some approved drugs for medical use such as *Sitagliptin*, *Lorpiprazole*, *Dapiprazole*, *Estazolam*, alprazolam and *triazolam*[7,8] (Fig. 1). In addition, quinoxaline derivatives were among the most important class of heterocyclic compounds due to their potent therapeutic applications including anticancer, anti-HIV, antiviral, anti-inflammatory, antibacterial, antiallergic, antioxidant, … *etc.*[9–11] Interestingly, *Erdafitinib* and *Brimodine* are quinoxaline-based commercial drugs in the market[12,13] (Fig. 1). The bis-carboxamide function also constituted a main structural-unit of some commercial medicines such as *Lacosamide* and *Batimastat* (Fig. 1). In addition, some bis-amide derivatives were found to have potent anticancer activities.[14–16]

The biological potencies of the fused systems: 1,2,4-triazolo[,3,4-*b*]thiadiazines, were broadly described in the literature.[17] Some 1,2,4-triazolo[3,4-*b*]thiadiazine scaffolds had promising anticancer activities against several human cancer cell lines without obvious signs of toxicity.[18–24] Interestingly, a list of

[a]*Department of Chemistry, Faculty of Science, Cairo University, Giza, 12613, Egypt. E-mail: ashrafabbas@cu.edu.eg; kmdawood@sci.cu.edu.eg; Fax: +202 35727556; Tel: +202 35676602*

[b]*Department of Chemistry, Faculty of Science, Suez Canal University, Ismailia, 41522, Egypt*

† Electronic supplementary information (ESI) available. See https://doi.org/10.1039/d2ra03549a

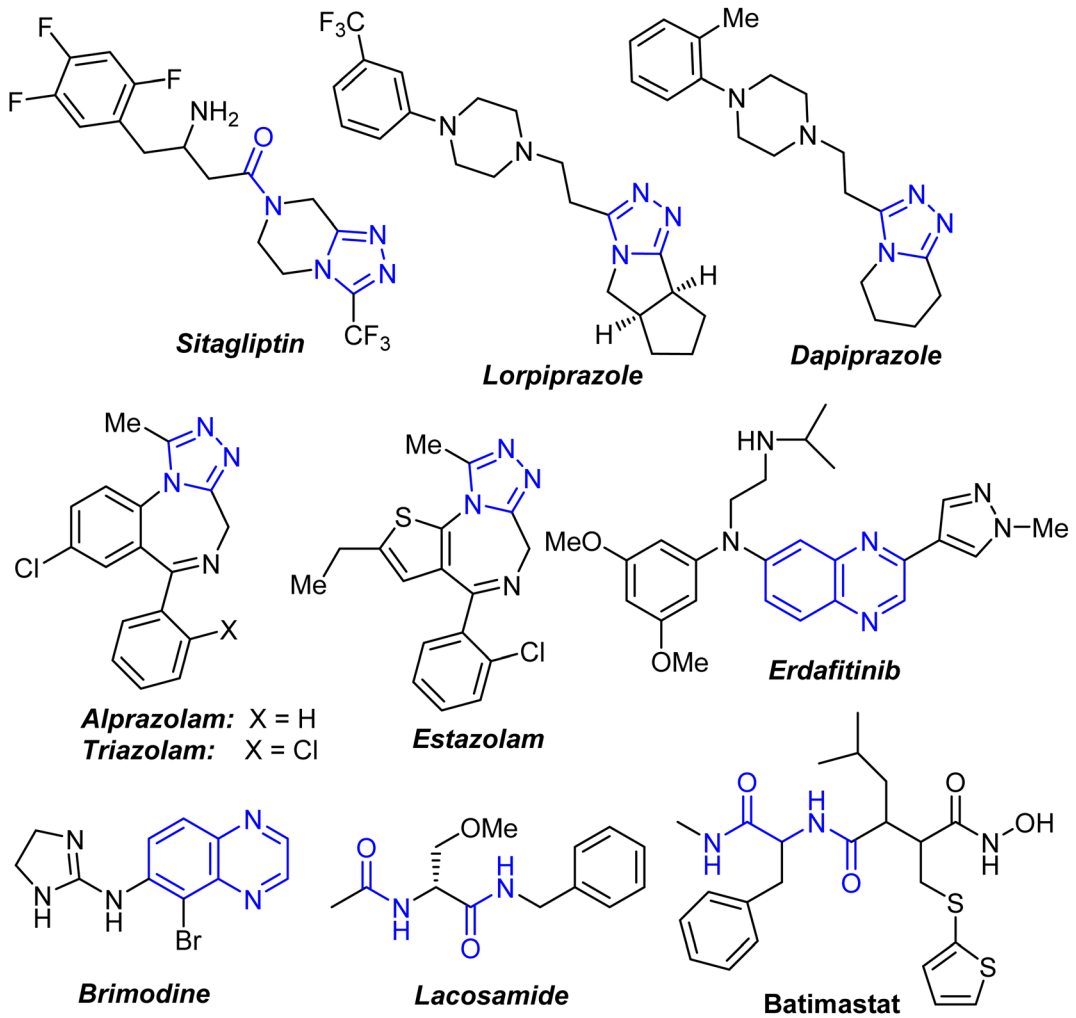

Fig. 1 Marketed-drugs based on carboxamides, fused-triazoles and quinoxalines.

triazole, thiadiazole and quinoxaline-based compounds with promising EGFR and PARP-1 inhibition is described in Fig. 2, hence, we thought to employ these moieties as an approach of fragment-based drug design. The 1,2,4-triazole derivative (**I**)[25] exhibited a promising cytotoxic activity as EGFR inhibitor with IC_{50} value of 1.5 μM, another derivative (**II**)[26] containing a 1,2,4-triazole moiety showed an interesting cytotoxic activity with apoptosis-induction through PARP-1 inhibition with IC_{50} value of 0.33 μM. The 1,2,4-triazolo[3,4-*b*]thiadiazine derivatives **III**[27] and **IV**[28] exhibited promising cytotoxic activities through EGFR and PARP-1 inhibitions with apoptosis-induction in cancer cells, respectively. Additionally, quinoxaline derivatives **V**[29] and **VI**[30] exhibited potent cytotoxicity against cancer cells, with inhibitory activities of EGFR (IC_{50} = 211.2 nM), and PARP-1 (IC_{50} = 71 nM).

Poly(ADP-ribose) polymerase (PARPs) are enzymes that catalyse the transfer of ADP-ribose from nicotinamide adenine dinucleotide (NAD+) to acceptor proteins.[31] PARP-1 is the most common and well-studied member of this family, and it represents a prospective anticancer therapeutic target as it is involved in DNA repair and cell survival and death.[32] Many researchers are interested in developing novel PARP-1 inhibitors, which showed promising effects in clinical studies against cancer. Epidermal growth factor receptor (EGFR) is a critical receptor that begins downstream signal transduction and causes tumor proliferation and migration, so its inhibition is a prospective cancer treatment target.[33]

Anticancer effects have been documented for 1,2,4-triazoles,[34] quinoxalines,[35] and 1,2,4-triazolo[3,4-*b*]thiadiazines,[27,28] that all work in various ways. They work by inhibiting the enzymes including PARP-1 and EGFR, which are involved in cancer progression. For newly synthesized bioactive compounds, molecular hybridization, *via* combination of two or more pharmacophoric motifs in the same substrate, was recommended to enhance their biological potencies.[36–38]

A subtype of breast cancer known as triple-negative (TNBC) was particularly dangerous and aggressive, with only few treatment options available.[39] EGFR has been found to be overexpressed in most cancers, including TNBC. For cancer treatment, the use of a PARP-1 inhibitor as a single target received considerable attention, but the potential of PARP in combination with other oncogenic targets was also accrued in recent

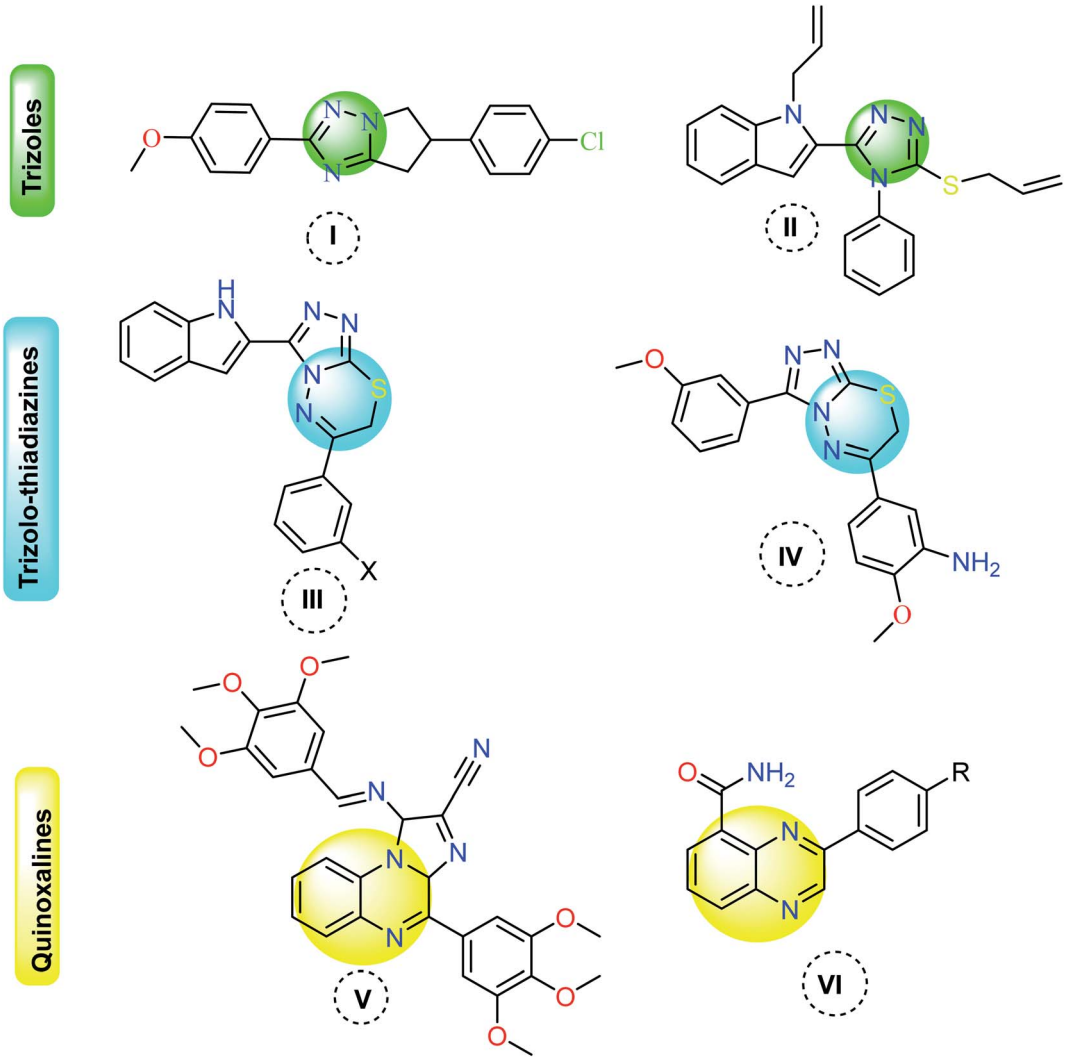

Fig. 2 Examples of triazole, thiadiazine and quinoxaline-based compounds as EGFR and PARP-1 inhibitors.

years. Other oncogenic targets such as EGFR could be used in conjunction with PARP.[40] Lin *et al.* 2022,[41] designed a potential PARP/EGFR dual inhibitor through pharmacophore combination using Olaparib as a clinically approved drug for PRAP-1 inhibitor. Additionally, PARP-1 inhibitors showed selective sensitivity to EGFR, hence dual inhibition targets of PARP-1/EGFR were a promising therapeutic target against cancers including breast cancer.[42]

Analyzing the receptor ligand-binding pocket and fragment interaction with pocket amino acid side chains using fragment-based drug design (FBDD) was a critical step in developing druggable lead structures. FBDD employed computer models of the target protein to narrow the search for possible leads, and these fragments served as the starting points for "growing" the lead candidate,[43,44] we thought to employ triazole, thiadiazine and quinoxaline-moieties as twin drugs against EGFR and PARP-1 proteins. It has been widely reported that functional agents combining two pharmacophoric groups in a single molecule (Twin drugs) have been effective in a wide range of medicinal chemistry applications.

During our research program aiming at synthesis of triazole-based fused heterocycles, bis(carboxamides) and bis(heterocycles) as twin drugs of significant biological applications,[45–55] the reported anticancer activities of compounds employing either triazolothiadiazine or carboxamide pharmacophores inspired us to construct a series of modified novel bis-triazolothiadiazine hybrids (Fig. 3) having variable bis(carboxamide) spacers, starting from bis(2-chloroacetamide) derivatives, to investigate their potency as anticancer agents against a panel of cancer cell lines and to investigate the effective molecular target and the apoptotic cell death.

2. Results and discussion

2.1. Chemistry

The activated bis-(2-chloroacetamide) derivatives **3a–c** were firstly prepared by conventional double *N*-alkylation of the readily available aliphatic 1,ω-diamino-alkanes **2a–c** with the highly reactive chloroacetyl chloride **1** following a procedure reported in the literature[56] (Scheme 1). The obtained bis-chloro

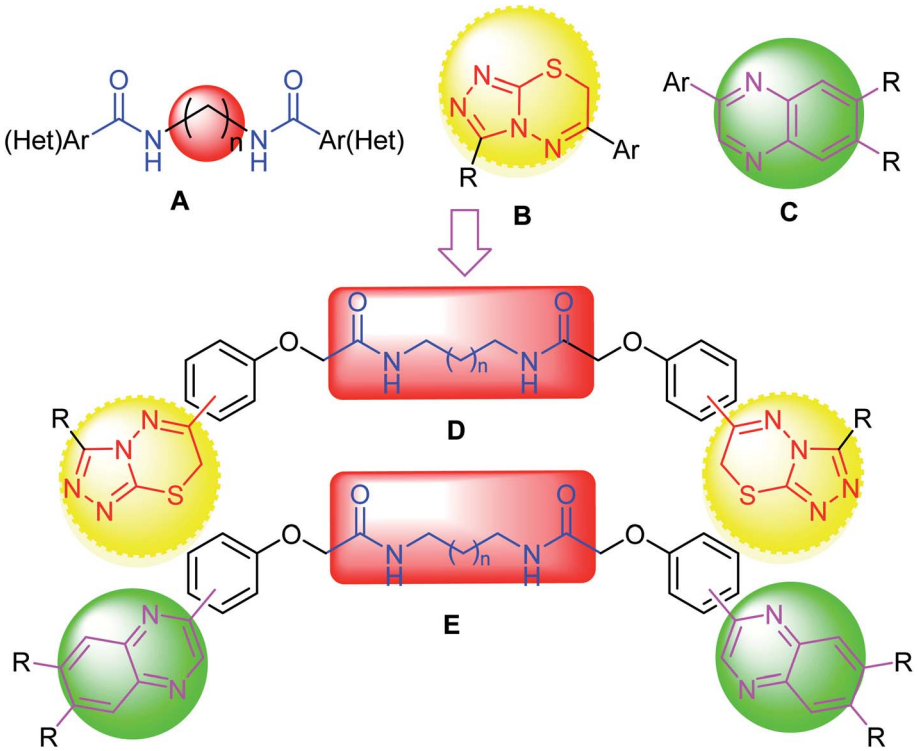

Fig. 3 Design strategy of our target; triazolothiadiazine or quinoxaline merged bis-carboxamide pharmacophores.

compounds **3a–c** were then used to alkylate the potassium salts of *p*-hydroxyacetophenone **4a** and its *o*-isomer **4b** [obtained upon treatment of hydoxyacetophenone derivatives **4a, b** with methanolic potassium hydroxide solution] in boiling DMF to afford the corresponding 1,ω-bis((acetylphenoxy)acetamide) alkanes **5a–f** in 60–65% yields as depicted in Scheme 1. Thus, reaction of one equivalent of *N*,*N*′-(ethane-1,2-diyl)bis(2-chloroacetamide) **3a** with two equivalents of the potassium salt of *p*-hydroxyacetophenone **4a** in boiling dimethylformamide (DMF) delivered the new bis(carboxamide); *N*,*N*′-(ethane-1,2-diyl)bis(2-(4-acetylphenoxy)acetamide) **5a** in 65% yield. Structure of the new product **5a** was fully confirmed from its elemental and spectral analyses (IR and ^{1}H NMR). The ^{1}H NMR spectrum of **5a** recorded a singlet signal at 2.49 for two acetyl protons, and two singlet peaks at 3.25 and 4.55 assignable to CH_2N and CH_2O protons, two doublets at 7.03 and 7.90 due to the *p*-phenylene aromatic protons, besides a singlet peak at 8.22 ppm assignable to NH function, respectively. Moreover, the IR spectrum of **5a** showed two sharp absorption peaks at 3286 and 1665 cm^{-1} assigned for NH and CO groups, respectively. Similarly, compounds **3b, c** reacted with the potassium salt of *p*-hydroxyacetopheneone **4a** and *o*-hydroxyacetopheneone **4b**, under the same reaction conditions, to furnish the corresponding *N*,*N*′-(alkane)bis(2-bromoacetyl)phenoxy)acetamides **5b–f** in 60–65% yields, as shown in Scheme 1. Structures of all the new bis(acetylphenoxy)acetamide)alkane derivatives **5b–f** were completely confirmed from both elemental and spectral analyses (IR, ^{1}HNMR and ^{13}CNMR) (*c.f.* Experimental section). The formed bis(acetyl) derivatives **5a–g** were characterized by the presence of an elongated spacer between the two carboxamide groups as well as the position of acetyl moiety on the aromatic ring.

Next, the bis-carboxamide-based bis(acetyl) derivatives **5a–f** were chosen as key compounds for preparation of the *hitherto* unreported *N*,*N*′-(alkane)bis(2-bromoacetyl)phenoxy) acetamides **6a–f** which were useful for synthesis of the target bis(heterocycles) in our project. Two strategies were attempted to synthesize the bis(2-bromoacetyl) derivatives **6a–f**. The first involved conventional direct bromination of **5a** with bromine in acetic acid as solvent at room temperature, however, this method led to the formation of a mixture of bis(α-bromoketone) **6a** and its bis(α,α-dibromoketone) derivatives as shown by TLC and ^{1}H NMR of the crude reaction mixture. The mixture was difficult to be separated into the corresponding pure products. In anticipation of getting an efficient and modified protocol to synthesize a pure sample of **6a**, an alternative synthetic way was attempted. Thus, bromination of the model compound **5a** with *N*-bromosuccinimide (NBS) catalyzed by *p*-toluenesulfonic acid (*p*-TsOH) in acetonitrile as solvent resulted in the formation of the desired bis(α-bromoketone) **6a** as a single pure product in 60% yield as proved by the ^{1}H NMR and TLC of the crude product (Scheme 1). ^{1}H NMR spectrum of the pure compound **6a** showed all the expected features with signals at δ 3.24–3.26 (m, 4H, 2CH_2N), 4.57 (s, 4H, 2CH_2O), 4.94 (s, 4H, 2CH_2Br), 7.05 (d, 4H, J = 8.7 Hz, ArH's), 8.04 (d, 4H, J = 9 Hz, ArH's), and 8.26 (s, 2H, 2NH) ppm. This result stimulated us to generalize this protocol to prepare the rest bis(α-bromoketone) derivatives **6b–f**. Thus, double bromination of **5b–f** with NBS, under typical

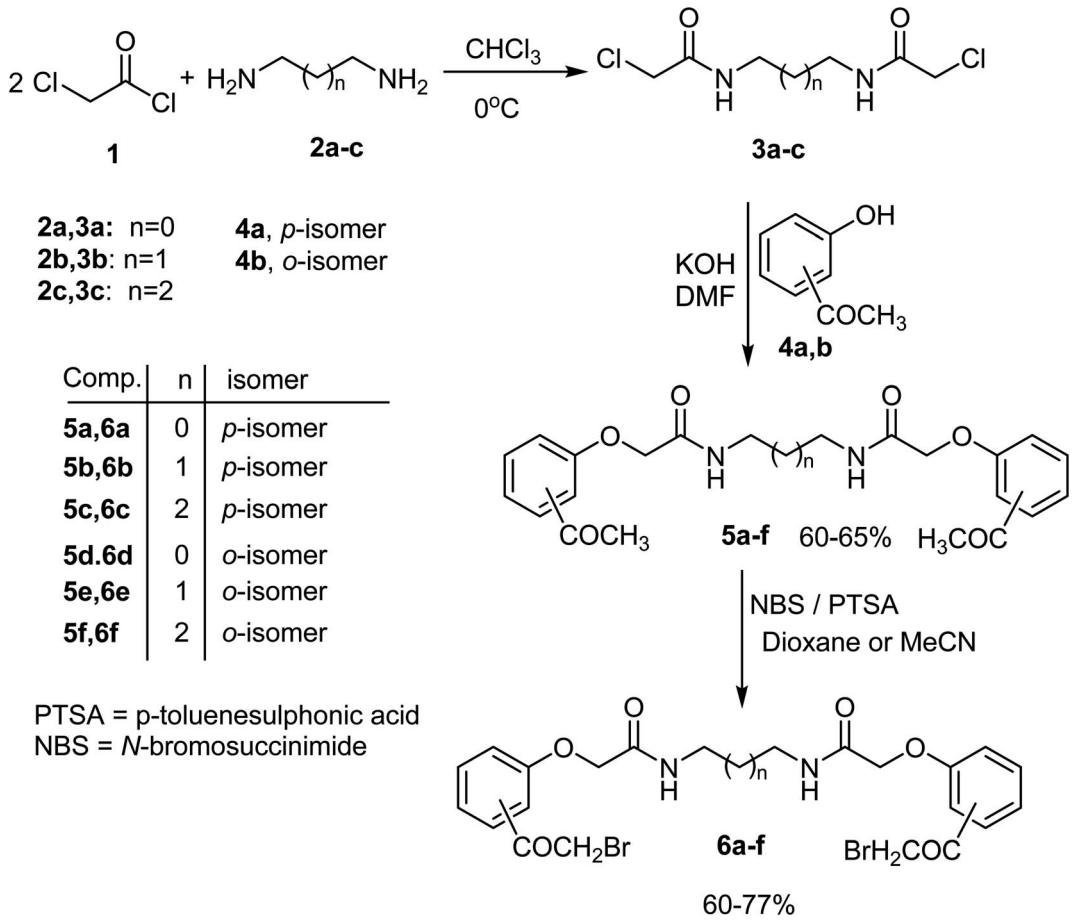

Scheme 1 Synthesis of *N,N′*-(alkane)bis((2-bromoacetyl)phenoxy)acetamides **6a–f**.

reaction condition, led to the formation of the desired compounds **6b–f** in 66–77% yields (Scheme 2). It is noteworthy to mention here that trials to improve the reaction yield, taking compound **6b** as a representative example, by switching the reaction solvent into dioxane instead of acetonitrile under the same reaction conditions failed, where compound **6b** was isolated in only 37% yield.

Next, our target was expanded to investigate the synthetic potentiality of the bis[((2-bromoacetyl)phenoxy)alkanamide] derivatives **6a–f** to access the bis[((1,2,4-triazolo[3,4-*b*][1,3,4] thiadiazin-6-yl)phenoxy)alkanamide] derivatives **8a–l**. Firstly, reaction of **6a** with two equivalents of 4-amino-5-phenyl-4*H*-1,2,4-triazole-3-thiol (**7a**) in refluxing ethanol, in the presence of a catalytic amount of piperidine, for 8 h afforded a low yield (30%) of *N,N′*-(ethane-1,2-diyl)bis(2-(4-(3-phenyl-7*H*-[1,2,4]triazolo[3,4-*b*][1,3,4]thiadiazin-6-yl)phenoxy)-acetamide) (**8a**). The low yield of **8a** might be attributed to the fair solubility of the starting materials in the reaction solvent (ethanol). Repeating the same reaction in DMF/ethanol mixed solvent (4 : 1 v/v) at reflux temperature, in the presence of piperidine, for 3 h furnished the desired product **8a** in 62% yield. The structure of **8a** was elucidated by elemental analyses, as well as its spectral data (^{1}H NMR, MS and IR), that were in complete accordance with the proposed structure **8a** (Scheme 2). The ^{1}H NMR spectrum of **8a** showed characteristic multiplet signals at δ 3.27 for CH_2N integrating for four protons, two singlet signals at δ 4.36 and 4.57 corresponding to CH_2S and CH_2O protons, respectively, multiplet signals in the region 7.11–8.01 for the aromatic protons in addition to a singlet signal at 8.23 ppm for two NH protons. Its IR spectrum showed characteristic sharp absorption peaks for NH and CO at ν 3433 and 1666 cm^{-1}, respectively. Finally, its mass spectrum showed a fragment at *m*/*z* 755 due to the correct molecular ion peak.

The above reaction was generalized where treatment of the appropriate bis(α-bromoacetophenone) **6a–f**, with two equivalents of the 4-aminotriazole-3-thiol derivatives **7a–d** under the same reaction conditions afforded the corresponding bis(-triazolothiadiazine) derivatives **8a–l** in 52–72% yields as shown in Scheme 2. The structures of the obtained products **8a–l** were substantiated from their elemental analyses and spectral data (^{1}H and ^{13}C NMR, MS and IR) as described in the experimental part. Mechanistically, formation of **8** took place *via* initial *S*-alkylation of the thiol group of aminotriazole-thiol with loss of two HBr molecules, followed by an intramolecular cyclocondensation with concurrent extrusion of two water molecules to furnish the product **8**. Strong evidence for the proposed mechanism was based on the following remarks; (a) disappearance of the characteristic signals NH_2 belong to amino-

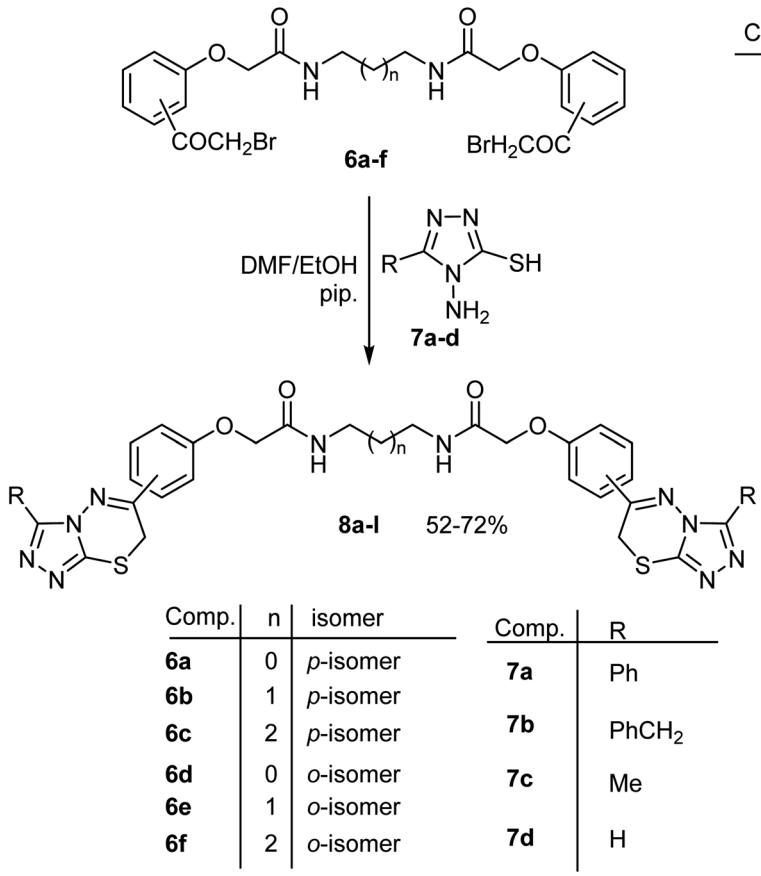

Comp.	Isomer	n	R
8a	*p*-	0	Ph
8b	*p*-	0	$PhCH_2$
8c	*o*-	0	Ph
8d	*o*-	0	Me
8e	*p*-	1	Ph
8f	*p*-	1	Me
8g	*o*-	1	Ph
8h	*o*-	1	$PhCH_2$
8i	*o*-	1	Me
8j	*p*-	2	Ph
8k	*o*-	2	Ph
8l	*o*-	2	H

Comp.	n	isomer
6a	0	*p*-isomer
6b	1	*p*-isomer
6c	2	*p*-isomer
6d	0	*o*-isomer
6e	1	*o*-isomer
6f	2	*o*-isomer

Comp.	R
7a	Ph
7b	$PhCH_2$
7c	Me
7d	H

Scheme 2 Synthesis of the bis(triazolothiadiazine) derivatives 8a–l.

triazole moiety in both IR and ^{1}H-NMR spectra of all the products **8a–l**, (b) presence of new SCH_2 protons, resonating at $\delta \sim 4.3$ ppm as singlet signal integrating for four protons, which clearly indicated the occurrence of ring closure.

Finally, our work was extended to comprise synthesis of the new functionalized bis((quinoxalin-2-yl)phenoxy)alkane derivatives **10a–e**. Thus, when the bis(α-bromoketones) **6a**, **b**, **d**, **f** were allowed to react with two equivalents of *o*-phenylenediamine derivatives **9a**, **b** in absolute ethanol containing piperidine (two equiv.), at reflux temperature, gave the corresponding bis(quinoxalin-2-yl)phenoxy)alkane derivatives **10a–d** in 50–70% yields as shown in Scheme 3. The structures of the isolated products were inferred from their elemental and spectral analyses as described in detail in the experimental part. For example, the spectral data (IR, ^{1}H- and ^{13}C-NMR and MS) of the bis(quinoxaline) derivative **10e** was interpreted in detail. The mass spectrum of **10e** showed the correct molecular ion peak at $m/z = 668$, and its IR spectrum revealed distinctive stretching absorption peaks at 3240, 1674 and 1620 cm^{-1} corresponding to NH, CO and C=N functions, respectively. The ^{1}H NMR of **10e** showed three singlet signals at δ 1.29, 2.46, 4.59 for four groups of CH_3 protons, CH_2CH_2NH, and OCH_2 protons, respectively, multiplet signals in the range 3.19–3.21 for four protons of $NHCH_2CH_2CH_2CH_2NH$, in addition to a singlet peak at δ 8.93 integrated for two protons referring to quinoxaline-3-C*H* and all the remaining protons appeared at the expected chemical shifts with correct integral values (see experimental part). The ^{13}C-NMR spectrum of **10e**, using APT technique, showed two signals at δ 20.35 and 20.41 for two CH_3 groups, three signals at 26.45, 38.35 and 67.61 for three aliphatic *C*H's, seven signals at 112.79, 122.52, 127.73, 127.78, 131.38, 131.54 and 144.83 for seven aromatic *C*H's, besides eight signals at 126.48, 139.74, 140.46, 140.69, 141.10, 150.27, and 154.85 for seven aromatic *C*'s and 167.91 for C=O group. Formation of the bis(quinoxaline) derivatives **10a–e** took place *via* initial nucleophilic attack at the bromoacetyl moiety followed an intramolecular cyclization *via* consecutive elimination of two molecules of water and finally aromatization *via* air oxidation to afford bis(quinoxalin-2-yl)phenoxy)alkane derivatives **10a–e**.

2.2. Biology

2.2.1. Cytotoxic activity of the synthesized molecules against breast cancer cell lines. The synthesized compounds were screened for their cytotoxicity against two breast cancer cell lines; MCF-7 and MDA-MB-231 using the MTT assay and the IC_{50} values were summarized in Table 1. As seen in the results, compounds **8d**, **8i** and **8l** exhibited cytotoxic activities with potent IC_{50} values of 0.41, 0.12, and 0.86 μM against MDA-MB-231 cells and IC_{50} values of 2.14, 1.31, and 5.31 μM against MCF-7 cells compared to Erlotinib as a reference drug (IC_{50} = 1.02

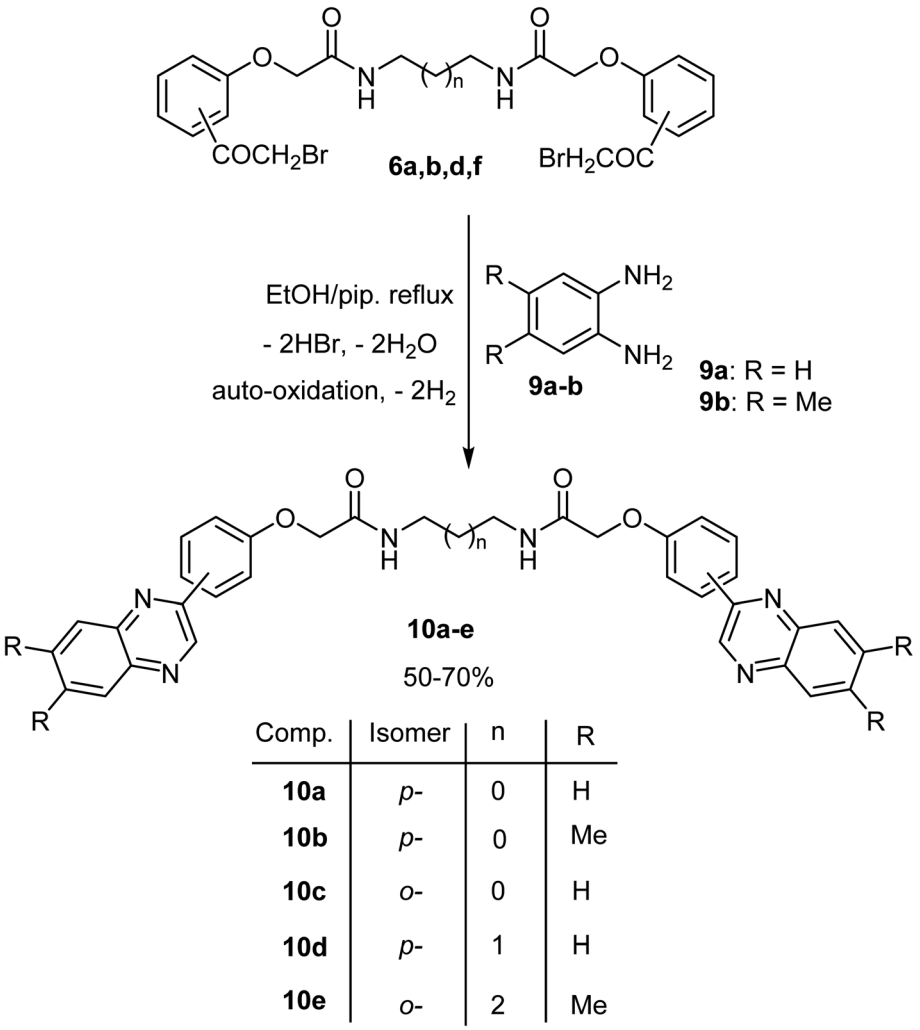

Comp.	Isomer	n	R
10a	*p*-	0	H
10b	*p*-	0	Me
10c	*o*-	0	H
10d	*p*-	1	H
10e	*o*-	2	Me

Scheme 3 Synthesis of the bis((quinoxalin-2-yl)phenoxy)alkane derivatives **10a–e**.

Table 1 Cytotoxicity of the synthesized compounds against the breast cancer MCF-7 and MDA-MB-231 cell lines using MTT assay[a]

	IC_{50}, μM			IC_{50}, μM	
No.	MCF-7	MDA-MB-231	No.	MCF-7	MDA-MB-231
8a	≥50	31.7	**10a**	32	≥50
8b	26.1	29.2	**10b**	≥50	22.37
8c	16.1	23.3	**10c**	7.61	11.01
8d	2.14	0.421	**10d**	23.21	≥50
8e	12.7	10.9	**10e**	31.21	28.1
8f	7.12	3.01	Erlotinib	0.32	1.02
8g	11.20	8.01			
8h	21.1	≥50			
8i	1.31	0.12			
8j	14.9	15.01			
8k	13.1	12.7			
8l	5.31	0.86			

[a] IC_{50} values were calculated as the average of three independent trials using dose–response curve in GraphPad prism.

and 0.32 μM for MDA-MB-231 and MCF-7, respectively). The other compounds exhibited mild to weak cytotoxicity. Compound **8i**, as the most cytotoxic compound against the two tested cell lines, it was subjected to MCF-10A as normal cell lines and exhibited a poor cytotoxicity with an IC_{50} value of 52.4 μM, and it caused around 90% cell inhibition at the highest concentration 100 μM (Fig. 4). The obtained results disclosed the highest activity of compound **8i** against the two breast cancer cells in a selective way.

Biological results of the current investigation revealed that there was an increase in the potency of the cytotoxicity and enzyme inhibition results of the tested bis-heterocyclic derivatives compared to the reported results of the mono-heterocyclic derivatives of triazole, thiadiazine and quinoxaline compounds.[25–30] Therefore, synthesis of the current bis-fused derivatives was an added value towards the anticancer activity (Fig. 5).

It is noteworthy to mention that the current synthesized derivatives **8a–l** were characterized by variable alkane linkers between the two carboxamide groups from ethylene to butylene and the different substitution position of the

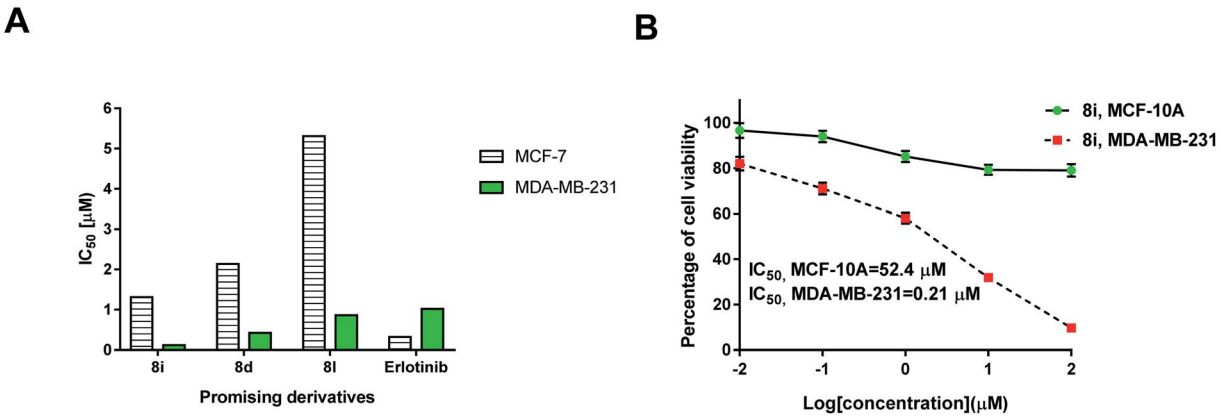

Fig. 4 (A) IC_{50} (μM) values of the promising derivatives **8i**, **8d**, and **8l** against MCF-7 and MDA-NB-231 cells compared to Erlotinib. (B) Cell viability of compound **8i** against breast cancer (MDA-MB-231) and normal breast (MCF-10A) cells using MTT assay for 48 h incubation.

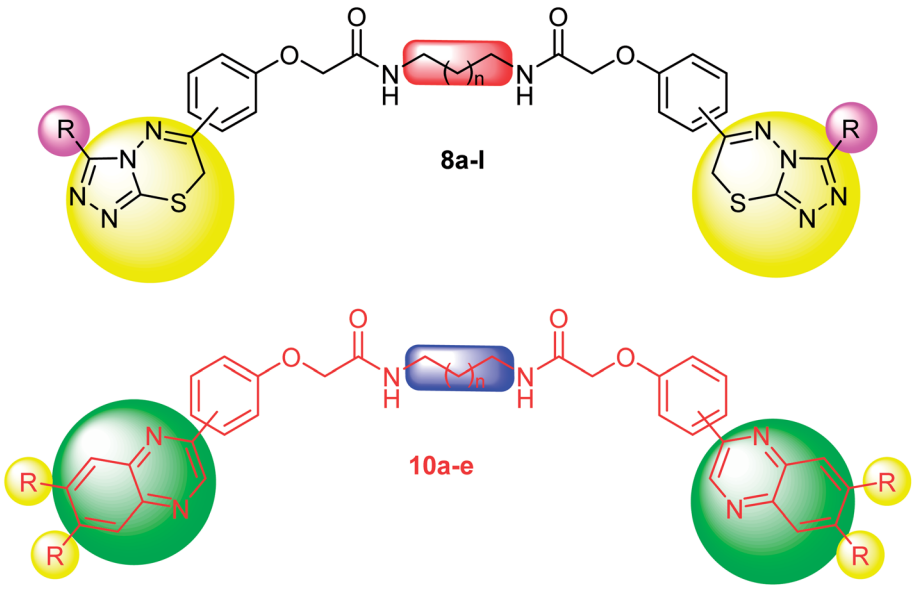

Fig. 5 Highlighted substituents anchored on the pharmacophore with promising cytotoxic activities for compounds **8a–l** and **10a–e**.

triazolothiadiazine or quinoxaline moieties to the aromatic phenylene ring (*ortho*- or *para*-) as well as the substituents at the triazole or quinoxaline rings themselves. Such variations were necessary to optimize the potency of the anticancer activity of the synthesized products.

As illustrated in Fig. 6, the biological screening of the mentioned compounds **8a–l** revealed a correlation between some compounds with comparable anticancer activity. Thus, compounds **8i**, **8d** and **8l** were the most active inhibitors of MDA-MB-231 cells with IC_{50} values 0.12, 0.421 and 0.86 μM, respectively. All these compounds **8i**, **8d** and **8l** had the triazolothiadiazinyl pharmacophore in the *ortho*-position of the phenylene group and had less bulky (Me or H) substituents at position 3 of the triazole scaffold. Interestingly, the most active lead compound was **8i** with the shortest alkane spacer (ethylene; where $n = 0$) between both bis-carboxamide groups. Thus, the anticancer potency was greatly affected by the presence of a less bulky group at triazole ring, and a short-length spacer (first level activity) as shown in Fig. 6. For the second level of activity (the *para*-isomeric series) shown in Fig. 6, a similar correlation between the bis-carboxamide having propylene spacer and methyl substituent at position 3 of triazole scaffold (**8f:** $IC_{50} = 3.01$ μM), was more active than those having phenyl group at position 3 of triazole scaffold with either propylene spacer (for **8g** and **8e**) or butylene spacer (for **8k**). Therefore, it was concluded that the most inhibitory active compounds were characterized by the following: (i) *ortho*-substitution was more potent than *para*-substitution, (ii) less bulky substituents at the triazole scaffold was more potent than others with phenyl moiety, (iii) shorter alkane spacer between the two carboxamide groups.

It was noticed that, among the bis-quinoxaline series **10a–e**, only three derivatives **10b**, **c**, **e** exhibited moderate anticancer activity in the order **10c** > **10b** > **10e** with IC_{50} values of 11.01,

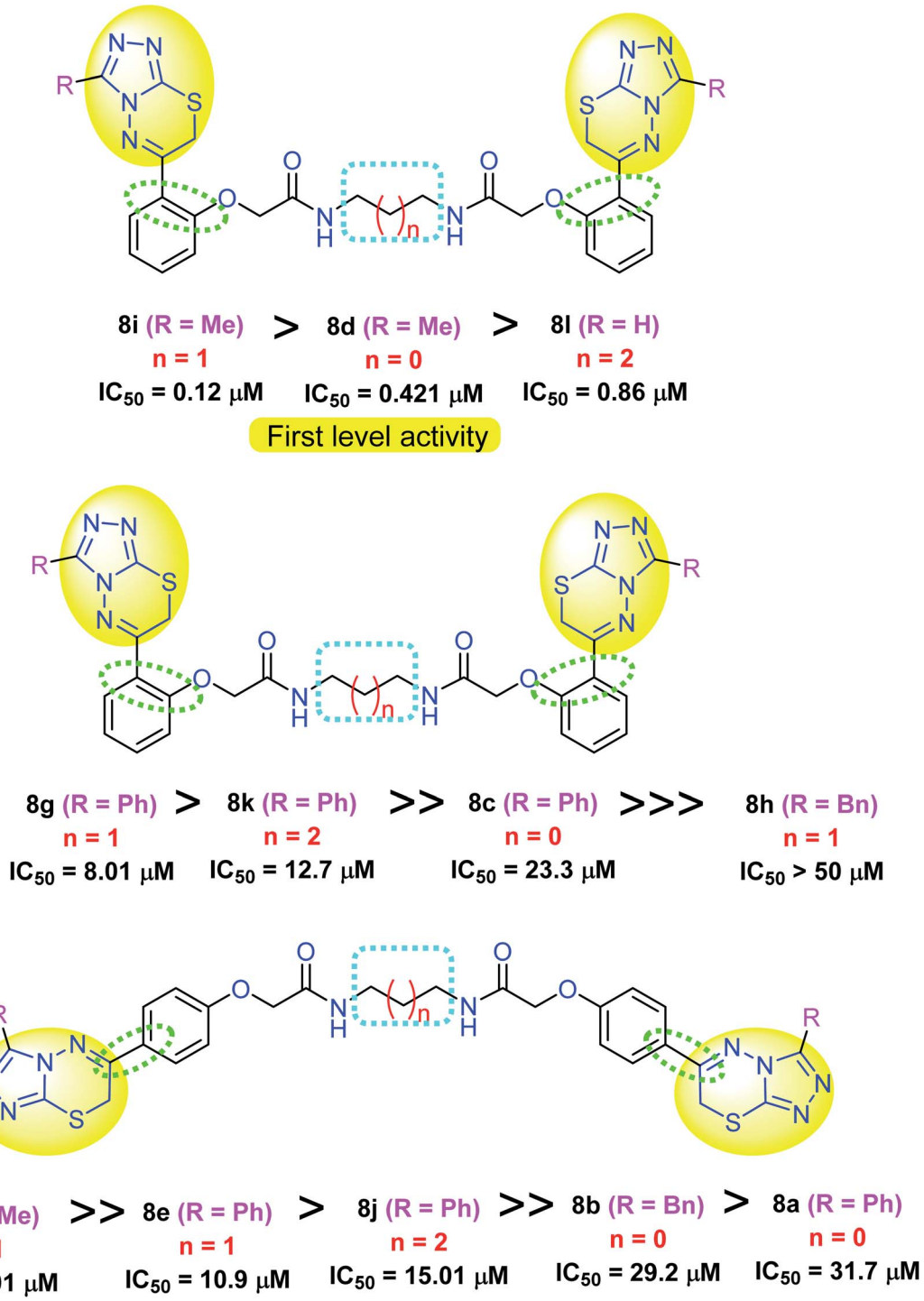

Fig. 6 Effect of derivatization of the synthesized bis-triazolothiadiazines **8a–l** on their cytotoxicity against MDA-MB-231 cells.

22.37 and 28.1 μM, respectively, against MDA-MB-231 cells. However, the other derivatives of the bis-quinoxaline series **10a, d** were totally inactive (IC_{50} > 50 μM).

2.2.2. Evaluation of PARP-1 and EGFR inhibitory activity. Compounds **8d**, **8i**, and **8l** were tested for their inhibitory activity on PARP-1 and EGFR as potential molecular targets, as seen in Table 2. Interestingly, compound **8i** exhibited promising dual enzyme inhibition PARP-1 with IC_{50} value of 1.37 nM compared to Olaparib (1.49 nM), and EGFR with IC_{50} value of 64.65 nM compared to Erlotinib (80 nM). While compound **8l** exhibited PARP-1 inhibitory activity with IC_{50} value of 6.87 nM, and EGFR inhibition with IC_{50} value of 78.9 nM. On contrast compound **8d** showed poor inhibitory activities. These results of dual PARP-1 and EGFR inhibition agreed with the previously reported results for 1,2,4-triazole, 1,3,4-thiadiazine and quinoxaline derivatives.[28–30]

Table 2 Dual EGFR-PARP enzymatic target of compound **8i**

	IC_{50}, nM[a]	
Sample	PARP-1	EGFR
8d	19.86	123.7
8i	1.37	64.65
8l	6.87	78.9
Erlotinib		80 (ref. 57)
Olaparib	1.49 (ref. 26)	

[a] IC_{50} values were calculated using sigmoidal nonlinear regression curve fit of percentage inhibition against five concentrations of each compound.

2.2.3. Effect of compound 8i on apoptosis in MDA-MB-231 cells using flow cytometry and RT-PCR assays. MDA-MB-231 cancer cells were treated with compound **8i** (IC_{50} = 0.12 μM, 48 h), and were investigated for their apoptosis-inducing activity using Annexin V/PI staining and DNA-aided cell cycle analysis with the cell population in different cell cycle phases. As seen in Fig. 7A, compound **8i** significantly stimulated total apoptotic breast cancer cell death with 38-fold (30.74% compared to 0.81% for the control). It induced early apoptosis by 11.23%, and late apoptosis by 19.51% compared to 0.63% and 0.18%, respectively, for the control. Moreover, it stimulated cell death by necrosis with 3.14-fold (4.08%, compared to 1.3% for the control).

Investigating at which cell cycle, cells were arrested while division, MDA-MB-231 cells were tested for cell cycle analysis, which indicated the cell population at each phase in both untreated and treated cells. As seen in Fig. 7B, compound **8i** significantly increased cell population at G2/M by 24.04%, compared to 9.83% for the control, so it arrested cell division at G2/M phase. Consequently, compound **8i** induced apoptosis in MDA-MB-231 cells arresting the cell cycle at G2/M.

Further validation of the apoptosis-inducing activity of the tested compound **8i** in MDA-MB-231 cells, the gene expression levels of apoptosis-related genes in both untreated and treated MDA-MB-231 cells were investigated through the RT-PCR. As seen in Fig. 8, compound **8i** treatment increased P53 level by 4.8-fold, Bax level by 4.46-fold, caspase-3 level by 3.9-fold, caspase-8 level by 6.36-fold, caspase-9 by 2.9-fold, while the

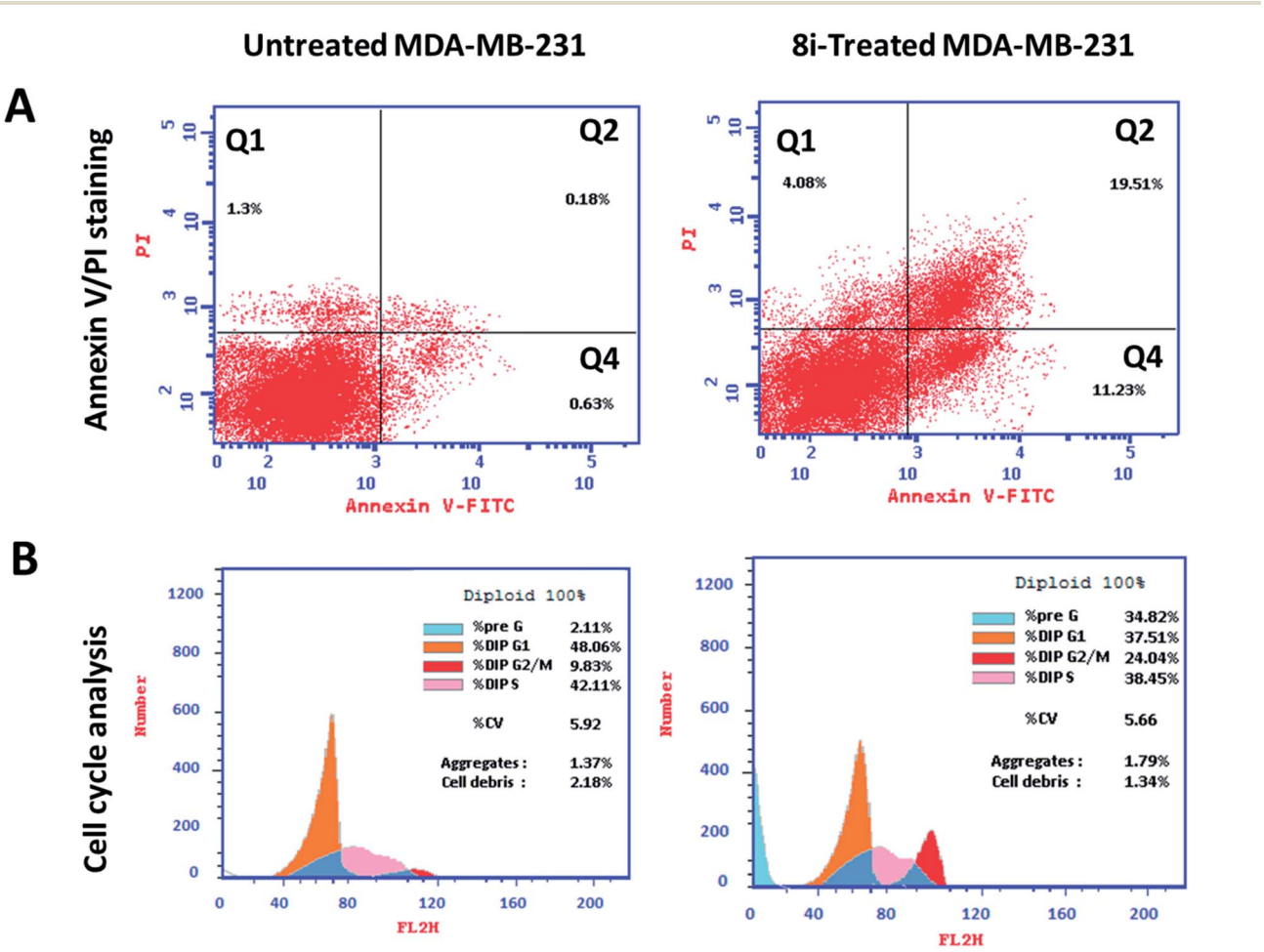

Fig. 7 Flow cytometry analysis upper panel (A) Annexin V/PI staining for apoptosis-necrosis assessment, (Q1) necrosis, (Q2) late apoptosis, (Q4) early apoptosis. Lower panel (B) histograms of DNA content at each phase of untreated and **8i**-treated MDA-MB-231 cells with IC_{50} value of 0.12 μM, 48 h.

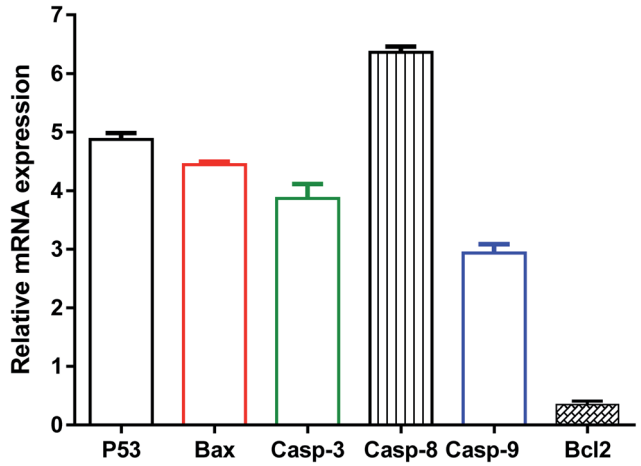

Fig. 8 Gene expression analysis in untreated and treated MDA-MB-231 cells at the IC_{50} of 0.12 μM, 48 h. Values are expressed as Mean ± SD for three independent experimental runs. The housekeeping gene is β-actin. Fold-change = $2^{\wedge-\Delta\Delta Ct}$, where ΔΔCt the difference between mean values of genes CT values in the treated and control groups. Fold of change in the untreated control = 1.

compound treatment decreased Bcl-2 level as the anti-apoptotic gene by 0.35-fold compared to the untreated control.

The activation of caspase-3,9 and the decreased expression of the Bcl-2 gene might cause apoptosis. P53 is a tumour suppressor gene that was essential for apoptosis. The results demonstrated the intrinsic apoptotic pathway *via* activation of P53, Bax, caspase 3 and 9. Furthermore, in treated MDA-MB-231 cells, increased caspase-8 gene expression favours the extrinsic apoptotic pathway. As a result, our findings agreed with previous studies that used RT-PCR to highlight the apoptotic pathway by upregulating proapoptotic genes and down-regulating anti-apoptotic genes.

2.2.4. Virtual justification of the biological investigations. Based on enzyme assay experimental results, the most active compound, **8i**, was screened for virtual binding towards PARP-1 and EGFR proteins and the docking data are summarized in Table 3. For PARP-1 protein the binding energy of **8i** was −37.09 kcal mol^{-1} compared with the co-crystallized ligand. The binding interaction take place through H-bond with Gly 863, H-bond with Ser 904, arene–cation with His 862, and arene–arene with Tyr 896. For the EGFR protein the binding energy of **8i** was −29.23 Kcal mol^{-1} compared with the co-

Table 3 :Ligand-receptor interactions of the docked compound **8i** with binding energies (kcal mol^{-1}) inside the PARP-1 and EGFR proteins

Target	Docking score (kcal mol^{-1})	3D Interactive pose[a]	Ligand–receptor interactions
PARP-1	−37.09	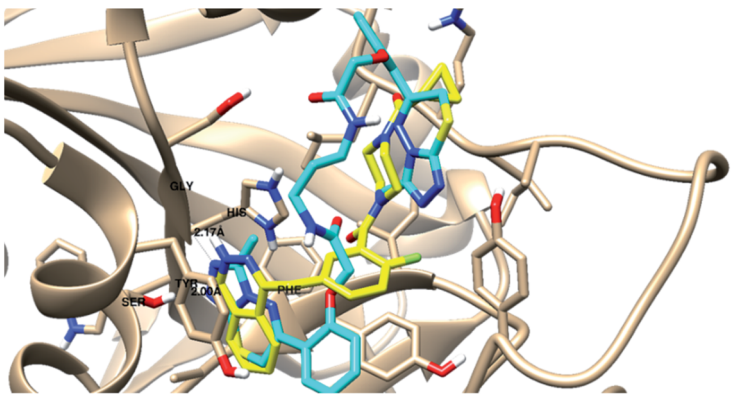	- 1 H-bond with Gly 863 - 1 H-bond with Ser 904 - 1 arene–cation with His 862 - 1 arene–arene with Tyr 896
EGFR	−29.23	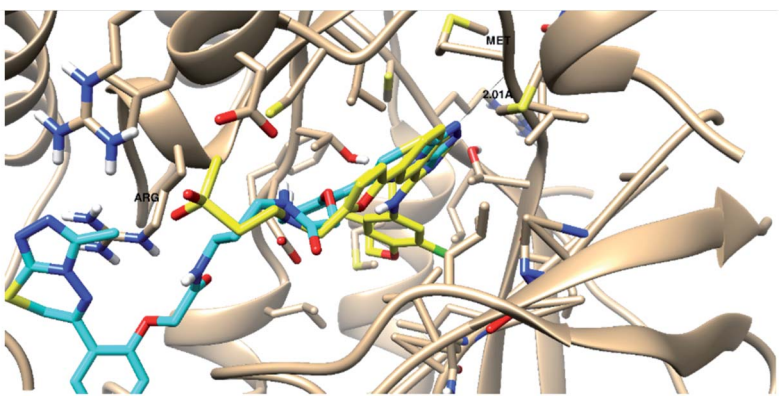	- 1 H-bond with Met793 - 1 arene–cation with Lys 745

[a] Binding disposition of compound **8i** (Cyan-colored) and co-crystallized ligands (Yellow-colored) inside the active sites of PARP-1and EGFR proteins. Labeled amino acids are the key ones for activity.

crystallized ligand. The binding interaction take place, however, through H-bond with Met 793 and arene–cation with Lys 745 as the key amino acids for enzyme activities. The docking results highlighted the rule of triazolo-thiadiazine moiety for interactions with targeted proteins PARP-1 and EGFR as illustrated by the 3D binding disposition. Further deep studies, however, requested for optimization of the activity and elucidation of the mode of actions of such type of molecules.

3. Conclusion

In this work, a synthetic protocol to a new series of bis((2-bromoacetyl)phenoxy)alkane derivatives linked by a bis-carboxaamide linker was developed and involved in the synthesis of a library of bis((triazolothiadiazinyl)phenoxy) alkane and bis((quinoxalin-2-yl)phenoxy)alkane derivatives *via* their reaction with 4-amino-1,2,4-triazole-3-thiol and *o*-phenylenediamine derivatives, respectively, in good yields. Structures of all the new compounds were established using elemental analyses and spectroscopic tools. The cytotoxicity of the synthesized compounds was tested using MTT assay, as well as apoptosis-induction through PARP-1 and EGFR as molecular targets. Compound **8i** exhibited high cytotoxic activity with IC_{50} values of 0.12 μM and 1.31 μM against MDA-MB-231 and MCF-7 cells, respectively, compared to Erlotinib. Interestingly, compounds **8i** induced apoptosis in MDA-MB-231 cells by 38-fold (30.74% compared to 0.81 for the control) arresting the cell cycle at G2/M phase, and it affected the apoptosis-related genes through RT-PCR. Additionally, compound **8i** exhibited promising dual enzyme inhibition PARP-1 (IC_{50} = 1.37 nM) compared to Olaparib (IC_{50} = 1.49 nM), and EGFR with (IC_{50} = 64.65 nM) compared to Erlotinib (IC_{50} = 80 nM). Hence, this compound may serve as a potential target-oriented anti-breast cancer agent.

4. Experimental

4.1. Chemistry

4.1.1. General methods. All melting points were uncorrected. Compounds prepared by different procedures were characterized by mixed melting points, thin-layer chromatography (TLC) and infra-red (IR). IR spectra (KBr) were recorded on Fourier Transform Infra-Red spectrophotometer: Model: IR-Affinity-1 from Shimadzu Corporation. Nuclear magnetic resonance (NMR) spectra were measured with a Varian Gemini 300 spectrometer (300 MHz ^{1}H NMR) and chemical shift were given in ppm from tetramethylsilane (TMS). ^{13}C NMR spectra were recorded with a Varian Mercury 300 (300 MHz ^{1}H NMR, 75 MHz ^{13}C NMR). Mass spectra were recorded on a DI Analysis Shimadzu QP-20100 Plus. Elemental analyses were carried out at the Microanalytical Centre, Cairo University. 4-Hydroxyacetophenone, 2-hydroxyacetophenone, chloroacetyl chloride, ethylene diamine, 1,3-diaminopropane, 1,4-diaminobutane, *N*-bromosuccinimide (NBS) and *p*-toluenesulfonic acid were used as purchased from Aldrich. The starting materials bis-(2-chloroacetamide)[56] **3a–c** were synthesized following the literature procedures.

4.1.2. Synthesis 1,ω-bis((acetylphenoxy)acetamide)alkanes 5a–f

4.1.2.1 General procedure. 4-Hydroxyacetophenone (**4a**) or 2-hydroxyacetophenone (**4b**) (10 mmol) was added to methanolic KOH solution [prepared by dissolving 0.56 g (10 mmol) of potassium hydroxide (KOH) in 10 mL of absolute methanol], stirred for 10 min and the solvent was then removed under *vacuum*. The obtained potassium salt was dissolved in DMF (10 mL) and the appropriate *N*,*N*′-(alkane-1,ω-diyl)bis(2-chloroacetamide) **3a–c** (5 mmol) was added. The reaction mixture was heated under reflux for 10 min during which KCl was precipitated. The solvent was then removed under *vacuum* and crushed ice was added to the reaction mixture. The obtained solid was collected by filtration, dried and recrystallized from EtOH/H_2O to afford bis(acetylphenoxy)alkanes **5a–f**.

*4.1.2.2 N,N′-(Ethane-1,2-diyl)bis(2-(4-acetylphenoxy) acetamide) (**5a**).* Obtained from **3a** and **4a**; colorless crystals; yield 65%, mp 176–178 °C; IR (KBr) ν 3286 (NH), 1666 (br, 2C=O) cm^{-1}; ^{1}H NMR (DMSO-d_6) δ 2.49 (s, 6H, 2CH_3CO), 3.25–3.26 (m, 4H, 2CH_2N), 4.55 (s, 4H, 2CH_2O), 7.03 (d, 4H, J = 9 Hz, ArH's), 7.90 (d, 4H, J = 8.7 Hz, ArH's), 8.22 (brs, 2H, 2NH) ppm. Anal. calcd for $C_{22}H_{24}N_2O_6$ (412.44): C, 64.07; H, 5.87; N, 6.79%. Found: C, 64.19; H, 5.90; N, 6.81%.

*4.1.2.3 N,N′-(Propane-1,3-diyl)bis(2-(4-acetylphenoxy) acetamide) (**5b**).* From **3b** and **4a**; colorless crystals, yield 64%, mp 134–136 °C; IR (KBr) ν 3387 (NH), 1658 (C=O) cm^{-1}; ^{1}H NMR ($CDCl_3$) δ 1.73 (quintet, 2H, J = 6 Hz, $CH_2CH_2CH_2$), 2.56 (s, 6H, 2CH_3CO), 3.36–3.42 (m, 4H, 2CH_2N), 4.56 (s, 4H, 2CH_2O), 6.99 (d, 4H, J = 8.7 Hz, ArH's), 7.20 (brs, 2H, 2NH), 7.95 (d, 4H, J = 8.7 Hz, ArH's) ppm; ^{13}C NMR ($CDCl_3$, APT) δ 26.18 (CH_3), 29.38, 35.35, 66.99, (3CH_2 aliphatic), 114.26, 130.56 (2CH, ArC's) 131.25, 166.72 (2C, ArC's), 167.91, 196.54 (2CO) ppm. Anal. calcd for $C_{23}H_{26}N_2O_6$ (426.47): C, 64.78; H, 6.15; N, 6.57%. Found: C, 64.85; H, 6.18; N, 6.66%.

*4.1.2.4 N,N′-(Butane-1,4-diyl)bis(2-(4-acetylphenoxy) acetamide) (**5c**).* From **3c** and **4a**; colorless crystals; yield 62%; mp 185–187 °C; IR (KBr) ν 3387 (NH), 1728, 1627 (C=O) cm^{-1}; ^{1}H NMR (DMSO-d_6) δ 1.41 (brs, 4H, 2CH_2CH_2N), 2.49 (s, 6H, 2CH_3CO), 3.11–3.13 (m, 4H, 2CH_2N), 4.55 (s, 4H, 2CH_2O), 7.03 (d, 4H, J = 8.7 Hz, ArH's), 7.91 (d, 4H, J = 8.7 Hz, ArH's), 8.12 (t, 2H, J = 5.7 Hz, 2NH), ppm. Anal. calcd for $C_{24}H_{28}N_2O_6$ (440.50): C, 65.44; H, 6.41; N, 6.36%. Found: C, 65.50; H, 6.45; N, 6.39%.

*4.1.2.5 N,N′-(Ethane-1,2-diyl)bis(2-(2-acetylphenoxy) acetamide) (**5d**).* From **3a** and **4b** gave crude **5d**; colorless crystals; yield 65%; mp 122–124 °C; IR (KBr) ν 3379 (NH), 1712, 1643 (C=O) cm^{-1}; ^{1}H NMR ($CDCl_3$) δ 2.46 (s, 6H, 2CH_3CO), 3.58–3.60 (m, 4H, 2CH_2N), 4.52 (s, 4H, 2CH_2O), 6.87 (d, 2H, J = 8.4 Hz, ArH's), 7.02 (t, 2H, J = 7.5 Hz, ArH's), 7.46 (t, 2H, J = 7.2 Hz, ArH's), 7.66 (d, 2H, J = 7.8 Hz, ArH's), 8.17 (brs, 2H, 2NH) ppm. Anal. calcd for $C_{22}H_{24}N_2O_6$ (412.44): C, 64.07; H, 5.87; N, 6.79%. Found: C, 64.19; H, 5.85; N, 6.90%.

*4.1.2.6 N,N′-(Propane-1,3-diyl)bis(2-(2-acetylphenoxy) acetamide) (**5e**).* From **3b** and **4b**; colorless crystals; yield 60%; mp 110–112 °C; IR (KBr) ν 3340 (NH), 1674, 1674 (C=O) cm^{-1}; ^{1}H NMR ($CDCl_3$) δ 1.88 (quintet, 2H, J = 6.3 Hz, $CH_2CH_2CH_2$), 2.61 (s, 6H, 2CH_3CO), 3.39–3.45 (m, 4H, 2CH_2N), 4.56 (s, 4H,

$2CH_2O$), 6.92 (d, 2H, J = 8.1 Hz, ArH's), 7.07 (t, 2H, J = 7.8 Hz, ArH's), 7.49 (t, 2H, J = 7.8 Hz, ArH's), 7.74 (d, 2H, J = 7.5 Hz, ArH's), 8.06 (brs, 2H, 2NH) ppm. Anal. calcd for $C_{23}H_{26}N_2O_6$ (426.47): C, 64.78; H, 6.15; N, 6.57%. Found: C, 64.69; H, 6.18; N, 6.65%.

*4.1.2.7 N,N′-(Butane-1,4-diyl)bis(2-(2-acetylphenoxy) acetamide) (**5f**).* From **3c** and **4b**; colorless crystals; yield 63%, mp 158–160 °C; IR (KBr) ν 3333 (NH), 1674 (C=O) cm^{-1}; ^1H NMR ($CDCl_3$) δ 1.68 (t, 4H, J = 2.7 Hz $2CH_2CH_2N$), 2.58 (s, 6H, $2CH_3CO$), 3.39–3.41 (m, 4H, $2CH_2N$), 4.54 (s, 4H, $2CH_2O$), 6.91 (d, 2H, J = 8.7 Hz, ArH's), 7.06 (t, 2H, J = 7.5 Hz, ArH's), 7.49 (t, 2H, J = 8.4 Hz, ArH's), 7.73 (d, 2H, J = 7.8 Hz, ArH's), 7.93 (brs, 2H, 2NH), ppm; ^{13}C NMR ($CDCl_3$, APT) δ 26.63, 38.59, 67.66 ($3CH_2$ aliphatic), 29.68 (CH_3), 113.49, 121.33, 131.11, 134.13 (4CH, ArC's) 127.03, 156.26 (2C, ArC's), 167.85, 198.81 (2CO) ppm. Anal. calcd for $C_{24}H_{28}N_2O_6$ (440.50): C, 65.44; H, 6.41; N, 6.36%. Found: C, 65.55; H, 6.49; N, 6.39%.

4.1.3. Synthesis of *N,N′*-((alkane)bis(2-bromoacetyl) phenoxy)acetamide) 6a–f

4.1.3.1 General procedure. To a stirred solution of the appropriate 1,ω-bis((acetylphenoxy)acetamide)alkanes **5a–f** (10 mmol) and *p*-toluenesulfonic acid monohydrate (*p*-TsOH) (5.7 g, 30 mmol) in acetonitrile (50 mL), was slowly added NBS (3.6 g, 20 mmol). After complete addition of NBS, the reaction mixture was refluxed with stirring for 3 h. The solvent was then removed under *vacuum* and the residue was left to cool to room temperature. Crushed ice (10 g) was added to the reaction mixture and the resulting mixture was stirred at 0 °C for 15 min. The solid product was collected by filtration, dried and recrystallized from the suitable solvent for each derivative to afford the corresponding bis(α-bromoketones) **6a–f**.

*4.1.3.2 N,N′-(Ethane-1,2-diyl)bis(2-(4-(2-bromoacetyl) phenoxy)acetamide) (**6a**).* Crystalized from dioxane as colorless crystals, yield 60%, mp 198–200 °C; IR (KBr) ν 3371 (NH), 1751, 1650 (C=O) cm^{-1}; ^1H NMR (DMSO-d_6) δ 3.24–3.26 (m, 4H, $2CH_2N$), 4.57 (s, 4H, $2CH_2O$), 4.94 (s, 4H, $2CH_2Br$), 7.05 (d, 4H, J = 8.7 Hz, ArH's), 8.04 (d, 4H, J = 9 Hz, ArH's), 8.26 (s, 2H, 2NH) ppm. Anal. calcd for $C_{22}H_{22}Br_2N_2O_6$ (570.23): C, 46.34; H, 3.89; N, 4.91%. Found: C, 46.41; H, 3.91; N, 4.93%.

*4.1.3.3 N,N′-(Propane-1,3-diyl)bis(2-(4-(2-bromoacetyl) phenoxy)acetamide) (**6b**).* Crystalized from dioxane as colorless crystals, yield 73%, mp 178–180 °C; IR (KBr) ν 3366 (NH), 1643 (C=O) cm^{-1}; ^1H NMR (DMSO-d_6) δ 1.59 (quintet, 2H, J = 6.6 Hz, $CH_2CH_2CH_2$), 3.10–3.17 (m, 4H, $2CH_2N$), 4.63 (s, 4H, $2CH_2O$), 5.47 (s, 4H, $2CH_2Br$), 7.05 (d, 4H, J = 8.7 Hz, ArH's), 8.03 (d, 4H, J = 9 Hz, ArH's), 8.21 (t, 2H, J = 5.7 Hz, 2NH) ppm. Anal. calcd for $C_{23}H_{24}Br_2N_2O_6$ (584.26): C, 47.28; H, 4.14; N, 4.79%. Found: C, 47.31; H, 4.19; N, 4.86%.

*4.1.3.4 N,N′-(Butane-1,4-diyl)bis(2-(4-(2-bromoacetyl) phenoxy)acetamide) (**6c**).* Crystalized from dioxane as colorless crystals, yield 70%, mp 162–164 °C; IR (KBr) ν 3294 (NH), 1643 (C=O) cm^{-1}; ^1H NMR (DMSO-d_6) δ 1.42 (s, 4H, $2CH_2CH_2N$), 3.12–3.13 (m, 4H, $2CH_2N$), 4.59 (s, 4H, $2CH_2O$), 4.82 (s, 4H, $2CH_2Br$), 7.07 (d, 4H, J = 9.3 Hz, ArH's), 7.98 (d, 4H, J = 8.7 Hz, ArH's), 8.15 (brs, 2H, 2NH) ppm. Anal. calcd for $C_{24}H_{26}Br_2N_2O_6$ (598.29): C, 48.18; H, 4.38; N, 4.68%. Found: C, 48.22; H, 4.45; N, 4.77%.

*4.1.3.5 N,N′-(Ethane-1,2-diyl)bis(2-(2-(2-bromoacetyl) phenoxy)acetamide) (**6d**).* Crystalized from ethanol/dioxane mixture as colorless crystals, yield 77%, mp 160–162 °C IR (KBr) ν 3294 (NH), 1674 (C=O) cm^{-1}; ^1H NMR ($CDCl_3$) δ 3.57–3.58 (m, 4H, $2CH_2N$), 4.44 (s, 4H, $2CH_2O$), 4.57 (s, 4H, $2CH_2Br$), 6.91 (d, 2H, J = 8.4 Hz, ArH's), 7.07 (t, 2H, J = 7.5 Hz, ArH's), 7.53 (t, 2H, J = 7.2 Hz, ArH's), 7.73 (d, 2H, J = 7.5 Hz, ArH's), 7.83 (brs, 2H, 2NH) ppm. Anal. calcd for $C_{22}H_{22}Br_2N_2O_6$ (570.23): C, 46.34; H, 3.89; N, 4.91%. Found: C, 46.39; H, 3.95; N, 4.99%.

*4.1.3.6 N,N′-(Propane-1,3-diyl)bis(2-(2-(2-bromoacetyl) phenoxy)acetamide) (**6e**).* Crystalized from ethanol as colorless crystals, yield 73%, mp 140–142 °C; IR (KBr) ν 3286 (NH), 1666 (C=O) cm^{-1}; ^1H NMR ($CDCl_3$) δ 1.79 (quintet, 2H, J = 6.3 Hz, $CH_2CH_2CH_2$), 3.33–3.39 (m, 4H, $2CH_2N$), 4.56 (s, 4H, $2CH_2O$), 4.62 (s, 4H, $2CH_2Br$), 6.95 (d, 2H, J = 8.4 Hz, ArH's), 7.11 (t, 2H, J = 7.5 Hz, ArH's), 7.55 (t, 2H, J = 7.2 Hz, ArH's), 7.75 (brs, 2H, 2NH), 7.80 (d, 2H, J = 7.8 Hz, ArH's) ppm; ^{13}C NMR ($CDCl_3$, APT) δ 29.06, 35.45, 35.67, 67.83 ($4CH_2$ aliphatic), 113.09, 121.84, 131.50, 135.07 (4CH, ArC's) 124.43, 156.66 (2C, ArC's), 167.97, 191.98 (2CO) ppm. Anal. calcd for $C_{23}H_{24}Br_2N_2O_6$ (584.26): C, 47.28; H, 4.14; N, 4.79%. Found: C, 47.10; H, 4.18; N, 4.65%.

*4.1.3.7 N,N′-(Butane-1,4-diyl)bis(2-(2-(2-bromoacetyl) phenoxy)acetamide) (**6f**).* Crystalized from ethanol as colorless crystals, yield 60%, mp 148–150 °C; IR (KBr) ν 3379 (NH), 1713 (C=O) cm^{-1}; ^1H NMR ($CDCl_3$) δ 1.64 (s, 4H, $2CH_2CH_2N$), 3.37–3.39 (m, 4H, $2CH_2N$), 4.47 (s, 4H, $2CH_2O$), 4.60 (s, 4H, $2CH_2Br$), 6.94 (d, 2H, J = 8.4 Hz, ArH's), 7.10 (t, 2H, J = 7.5 Hz, ArH's), 7.53 (brs, 2H, 2NH), 7.55 (t, 2H, J = 7.2 Hz, ArH's), 7.77 (d, 2H, J = 7.8 Hz, ArH's) ppm. Anal. calcd for $C_{24}H_{26}Br_2N_2O_6$ (598.29): C, 48.18; H, 4.38; N, 4.68%. Found: C, 48.28; H, 4.42; N, 4.75%.

4.1.4. Synthesis of the bis(triazolothiadiazine) derivatives 8a–l

4.1.4.1 General procedure. To a mixture of the appropriate bis(α-bromoacetophenone) derivative **6a–f** (5 mmol) and the appropriate aminotriazolethiol derivative **7a–d** (10 mmol) in DMF/absolute ethanol mixture (25 mL, 4 : 1, v/v), piperidine (10 mmol) was added and the mixture was heated under reflux for 8 h, then left to cool to room temperature. Crushed ice was (5 g) added to the reaction mixture and chest in the frig overnight. The resulting precipitate was collected by filtration, dried and recrystallized from the suitable solvent to afford the corresponding bis(fused-heterocyclic) derivatives **8a–l** in good yields.

*4.1.4.2 N,N′-(Ethane-1,2-diyl)bis(2-(4-(3-phenyl-7H-[1,2,4] triazolo[3,4-b][1,3,4]thiadiazin-6-yl)phenoxy)acetamide) (**8a**).* From **6a** and **7a**, crystallized from DMF as colorless crystals, yield 62%, mp 264–266 °C; IR (KBr) ν 3433 (NH), 1666 (C=O) cm^{-1}; MS *m*/*z* (%): 77 (73%), 104 (100%), 118 (87%), 177 (59%), 308 (2%), 365 (1.3%), 444 (2%), 568 (3%), 668 (3.2%), 705 (2%), (%), 755 ($M^+ - 1$, 1.5%); ^1H NMR (DMSO-d_6) δ 3.27 (m, 4H, $2CH_2N$), 4.36 (s, 4H, $2CH_2S$), 4.57 (s, 4H, $2CH_2O$), 7.11 (d, 4H, J = 8.1 Hz, ArH's), 7.55 (s, 6H, ArH's), 7.95 (d, 4H, J = 8.1 Hz, ArH's), 7.99–8.01 (m, 4H, ArH's), 8.23 (brs, 2H, 2NH) ppm. Anal. calcd for $C_{38}H_{32}N_{10}O_4S_2$ (756.86): C, 60.30; H, 4.26; N, 18.51%. Found: C, 60.39; H, 4.16; N, 18.59%.

*4.1.4.3 N,N′-(Ethane-1,2-diyl)bis(2-(4-(3-benzyl-7H-[1,2,4]tri-azolo[3,4-b][1,3,4]thiadiazin-6-yl)phenoxy)acetamide) (**8b**).* From

6a and **7b**, crystalized from DMF/ethanol as yellow crystals, yield 60%, mp 140–142 °C IR (KBr) ν 3194 (NH), 1666 (C=O) cm^{-1}; MS *m/z* (%): 91 (100%), 118 (45%), 313 (0.6%), 400 (0.5%), 457 (0.5%), 501 (1%), 601 (0.5%), 643 (0.5%), 699 (0.3%), 750 (0.3%), 784 (M^+, 0.2%); ^{1}H NMR (DMSO-d_6) δ 3.28 (s, 4H, $2CH_2N$), 4.26 (s, 4H, $2CH_2S$), 4.30 (s, 4H, $2CH_2Ph$), 4.56 (s, 4H, $2CH_2O$), 7.07 (d, 4H, J = 8.1 Hz, ArH's), 7.23 (m, 10H, ArH's), 7.93 (d, 4H, J = 8.4 Hz, ArH's), 8.24 (brs, 2H, 2NH) ppm. Anal. calcd for $C_{40}H_{36}N_{10}O_4S_2$ (784.91): C, 61.21; H, 4.62; N, 17.85%. Found: C, 61.05; H, 4.69; N, 17.69%.

*4.1.4.4 N,N′-(Ethane-1,2-diyl)bis(2-(2-(3-phenyl-7H-[1,2,4]triazolo[3,4-b][1,3,4]thiadiazin-6-yl)phenoxy)acetamide) (**8c**).* From **6d** and **7a**, crystalized from DMF/ethanol as yellow crystals, yield 60%, mp 240–242 °C IR (KBr) ν 3209 (NH), 1681 (C=O) cm^{-1}; MS *m/z* (%): 97 (61%), 149 (100%), 198 (20%), 322 (13%), 449 (13%), 593 (14%), 636 (15%), 707 (16%), 756 (M^+, 17%); ^{1}H NMR (DMSO-d_6) δ 3.24 (m, 4H, $2CH_2N$), 4.36 (s, 4H, $2CH_2S$), 4.63 (s, 4H, $2CH_2O$), 7.07–7.12 (m, 4H, ArH's), 7.51–7.60 (m, 10H, ArH's), 7.99 (m, 4H, ArH's), 8.08 (s, 2H, 2NH) ppm; ^{13}C NMR (DMSO-d_6) δ 25.42, 38.29, 67.37, 113.18, 121.11, 121.64, 124.17, 125.96, 127.89, 128.77, 130.27, 132.95, 143.02, 151.65, 156.28, 157.26, 167.61 ppm. Anal. calcd for $C_{38}H_{32}N_{10}O_4S_2$ (756.86): C, 60.30; H, 4.26; N, 18.51%. Found: C, 60.22; H, 4.14; N, 18.60%.

*4.1.4.5 N,N′-(Ethane-1,2-diyl)bis(2-(2-(3-methyl-7H-[1,2,4]triazolo[3,4-b][1,3,4]thiadiazin-6-yl)phenoxy)acetamide) (**8d**).* From **6d** and **7c**, crystalized from ethanol as yellow crystals, yield 61%, mp 240–242 °C; IR (KBr) ν 3263 (NH), 1674 (C=O) cm^{-1}; MS *m/z* (%): 97 (67%), 115 (100%), 130 (49%), 172 (21%), 246 (24%), 313 (11%), 447 (3%), 525 (3%), 604 (4%), 632 (M^+, 4%); ^{1}H NMR (DMSO-d_6) δ 2.44 (s, 6H, $2CH_3$), 3.23 (m, 4H, $2CH_2N$), 4.29 (s, 4H, $2CH_2S$), 4.61 (s, 4H, $2CH_2O$), 7.08–7.13 (m, 4H, ArH's), 7.50–7.59 (m, 4H, ArH's), 8.08 (s, 2H, 2NH); ^{13}C NMR (DMSO-d_6) δ 9.96, 25.65, 38.21, 67.32, 105.78, 113.09, 120.69, 124.28, 130.13, 132.81, 140.46, 145.46, 156.20, 167.55 ppm. Anal. calcd for $C_{28}H_{28}N_{10}O_4S_2$ (632.72): C, 53.15; H, 4.46; N, 22.14%. Found: C, 53.22; H, 4.52; N, 22.01%.

*4.1.4.6 N,N′-(Propane-1,3-diyl)bis(2-(4-(3-phenyl-7H-[1,2,4]triazolo[3,4-b][1,3,4]thiadiazin-6-yl)phenoxy)acetamide) (**8e**).* From **6b** and **7a**, crystalized from dioxane/ethanol as yellow crystals, yield 60%, mp 128–130 °C; IR (KBr) ν 3410 (NH), 1659 (C=O) cm^{-1}; MS *m/z* (%): 58 (100%), 77 (59%), 104 (71%), 121 (46%), 177 (21%), 192 (59%), 256 (5%), 368 (1.5%), 650 (1.5%), 743 (1%), 770 (M^+, 1%); ^{1}H NMR (DMSO-d_6) δ 1.62 (quintet, 2H, J = 6.6 Hz, $CH_2CH_2CH_2$), 3.05–3.20 (m, 4H, $2CH_2N$), 4.39 (s, 4H, $2CH_2S$), 4.60 (s, 4H, $2CH_2O$), 7.13 (d, 4H, J = 9 Hz, ArH's), 7.53–7.60 (m, 6H, ArH's), 7.96–8.03 (m, 8H, ArH's), 8.12 (t, 2H, J = 5.7 Hz, 2NH) ppm. Anal. calcd for $C_{39}H_{34}N_{10}O_4S_2$ (770.89): C, 60.76; H, 4.45; N, 18.17%. Found: C, 60.69; H, 4.49; N, 18.25%.

*4.1.4.7 N,N′-(Propane-1,3-diyl)bis(2-(4-(3-methyl-7H-[1,2,4]triazolo[3,4-b][1,3,4]thiadiazin-6-yl)phenoxy)acetamide) (**8f**).* From **6b** and **7c**, crystalized from ethanol as yellow crystals, yield 52%, mp 128–130 °C; IR (KBr) ν 3441 (NH), 1659 (C=O) cm^{-1}; MS *m/z* (%): 56 (28%), 115 (100%), 130 (5%), 303 (0.5%), 390 (0.2%), 451 (0.2%), 482 (0.3%), 523 (0.5%), 551 (0.3%), 604 (0.3%), 646 (M^+, 0.3%); ^{1}H NMR (DMSO-d_6) δ 1.61 (quintet, 2H, J = 6.6 Hz, $CH_2CH_2CH_2$), 2.46 (s, 6H, $2CH_3$), 3.10–3.20 (m, 4H, $2CH_2N$), 4.32 (s, 4H, $2CH_2S$), 4.59 (s, 4H, $2CH_2O$), 7.12 (d, 4H, J = 8.7 Hz, ArH's), 7.99 (d, 4H, J = 8.7 Hz, ArH's), 8.18 (t, 2H, J = 5.4 Hz, 2NH) ppm. Anal. calcd for $C_{29}H_{30}N_{10}O_4S_2$ (646.75): C, 53.86; H, 4.68; N, 21.66%. Found: C, 53.95; H, 4.75; N, 21.56%.

*4.1.4.8 N,N′-(Propane-1,3-diyl)bis(2-(2-(3-phenyl-7H-[1,2,4]triazolo[3,4-b][1,3,4]thiadiazin-6-yl)phenoxy)acetamide) (**8g**).* From **6e** and **7a**, crystalized from DMF as pale yellow crystals, yield 52%, mp 270–272 °C; IR (KBr) ν 3225 (NH), 1682 (C=O) cm^{-1}; MS *m/z* (%): 77 (71%), 91 (64%), 104 (100%), 118 (67%), 177 (69%), 192 (20%), 308 (14%), 495 (3%), 598 (3%), 732 (3%), 770 (M^+, 3%); ^{1}H NMR (DMSO-d_6) δ 1.57 (quintet, 2H, J = 6.6 Hz, $CH_2CH_2CH_2$), 3.10–3.16 (m, 4H, $2CH_2N$), 4.38 (s, 4H, $2CH_2S$), 4.60 (s, 4H, $2CH_2O$), 7.09–7.14 (m, 4H, ArH's), 7.51–7.61 (m, 10H, ArH's), 7.94–8.06 (m, 6H, 4ArH's & 2NH) ppm. Anal. calcd for $C_{39}H_{34}N_{10}O_4S_2$ (770.89): C, 60.76; H, 4.45; N, 18.17%. Found: C, 60.79; H, 4.55; N, 18.02%.

*4.1.4.9 N,N′-(Propane-1,3-diyl)bis(2-(2-(3-benzyl-7H-[1,2,4]triazolo[3,4-b][1,3,4]thiadiazin-6-yl)phenoxy)acetamide) (**8h**).* From **6e** and **7b**, crystalized from ethanol as yellow crystals, yield 62%, mp 202–204 °C; IR (KBr) ν 3287 (NH), 1682 (C=O) cm^{-1}; MS *m/z* (%): 77 (21%), 91 (100%), 191 (48%), 275 (7%), 415 (3%), 567 (3%), 674 (3%), 733 (3%), 798 (M^+, 2%); ^{1}H NMR ($CDCl_3$) δ 1.56 (brs, 2H, $CH_2CH_2CH_2$), 3.20–3.22 (m, 4H, $2CH_2N$), 3.99 (s, 4H, $2CH_2S$), 4.26 (s, 4H, $2CH_2Ph$), 4.29 (s, 4H, $2CH_2O$), 6.96–7.54 (m, 18H, ArH's), 7.56 (t, 2H, J = 7.2 Hz, 2NH) ppm. Anal. calcd for $C_{41}H_{38}N_{10}O_4S_2$ (798.94): C, 61.64; H, 4.79; N, 17.53%. Found: C, 61.51; H, 4.85; N, 17.59%.

*4.1.4.10 N,N′-(Propane-1,3-diyl)bis(2-(2-(3-methyl-7H-[1,2,4]triazolo[3,4-b][1,3,4]thiadiazin-6-yl)phenoxy)acetamide) (**8i**).* From **6e** and **7c**, crystalized from methanol as yellow crystals, yield 72%, mp 178–180 °C; IR (KBr) ν 3433 (NH), 1682 (C=O) cm^{-1}; MS *m/z* (%): 97 (31%), 115 (100%), 130 (75%), 172 (36%), 246 (12%), 304 (7%), 444 (4%), 465 (2%), 588 (5%), 646 (M^+, 3%); ^{1}H NMR ($CDCl_3$) δ 1.62 (brs, 2H, $CH_2CH_2CH_2$), 2.50 (s, 6H, $2CH_3$), 3.20–3.35 (m, 4H, $2CH_2N$), 4.07 (s, 4H, $2CH_2S$), 4.49 (s, 4H, $2CH_2O$), 7.03 (d, 2H, J = 8.4 Hz, ArH's), 7.15 (t, 2H, J = 7.5 Hz, ArH's), 7.49–7.58 (m, 6H, 4ArH's & 2NH) ppm. Anal. calcd for $C_{29}H_{30}N_{10}O_4S_2$ (646.75): C, 53.86; H, 4.68; N, 21.66%. Found: C, 53.92; H, 4.53; N, 21.82%.

*4.1.4.11 N,N′-(Butane-1,4-diyl)bis(2-(4-(3-phenyl-7H-[1,2,4]triazolo[3,4-b][1,3,4]thiadiazin-6-yl)phenoxy)acetamide) (**8j**).* From **6c** and **7a**, which was crystalized from DMF as yellow crystals, yield 72%, mp 260–262 °C; IR (KBr) ν 3280 (NH), 1659 (C=O) cm^{-1}; MS *m/z* (%): 77 (41%), 104 (59%), 118 (69%), 177 (100%), 375 (1%), 527 (2%), 620 (1.2%), 785 ($M^+ + 1$, %); ^{1}H NMR (DMSO-d_6) δ 1.43 (brs, 4H, CH_2CH_2N), 3.15 (s, 4H, $2CH_2NH$), 4.39 (s, 4H, $2CH_2S$), 4.58 (s, 4H, $2CH_2O$), 7.12 (d, 4H, J = 8.7 Hz, ArH's), 7.55–7.57 (m, 6H, ArH's), 7.95–8.03 (m, 8H, ArH's), 8.14 (t, 2H, J = 5.4 Hz, 2NH) ppm. Anal. calcd for $C_{40}H_{36}N_{10}O_4S_2$ (784.91): C, 61.21; H, 4.62; N, 17.85%. Found: C, 61.17; H, 4.72; N, 17.77%.

*4.1.4.12 N,N′-(Butane-1,4-diyl)bis(2-(2-(3-phenyl-7H-[1,2,4]triazolo[3,4-b][1,3,4]thiadiazin-6-yl)phenoxy)acetamide) (**8k**).* From **6f** and **7a**, crystalized from DMF as yellow crystals, yield 65%, mp 262–264 °C; IR (KBr) ν 3371 (NH), 1682 (C=O) cm^{-1}; MS *m/z* (%): 77 (62%), 118 (84%), 177 (100%), 308 (4%), 338 (2%), 442

(1.2%), 560 (1.5%), 618 (1.5%), 715 (2%), 784 (M^+, 1.2%); ^{1}H NMR (DMSO-d_6) δ 1.40 (brs, 4H, CH_2CH$_2$N), 3.10–3.12 (m, 4H, 2CH$_2$N), 4.39 (s, 4H, 2CH$_2$S), 4.67 (s, 4H, 2CH$_2$O), 7.08–7.13 (m, 6H, ArH's), 7.52–7.61 (m, 10H, ArH's), 7.98–8.01 (m, 4H, 2ArH's & 2NH) ppm; ^{13}C NMR (DMSO-d_6) δ 25.43, 26.50, 38.10, 67.48 (aliphatic C's), 113.19, 121.62, 124.18, 125.96, 127.89, 128.76, 130.25, 132.92, 142.99, 151.65, 156.38, 157.23, 167.09 (CO) ppm. Anal. calcd for $C_{40}H_{36}N_{10}O_4S_2$ (784.91): C, 61.21; H, 4.62; N, 17.85%. Found: C, 61.15; H, 4.66; N, 17.78%.

*4.1.4.13 N,N′-(Butane-1,4-diyl)bis(2-(2-(7H-[1,2,4]triazolo[3,4-b][1,3,4]thiadiazin-6-yl)phenoxy)-acetamide) (**8l**).* From **6f** and **7d**, crystalized from acetic acid/ethanol as yellow crystals, yield 72%, mp 132–134 °C; IR (KBr) ν 3240 (NH), 1674 (C=O) cm^{-1}; MS *m*/*z* (%): 101 (100%), 322 (22%), 363 (1.2%), 435 (0.2%), 483 (0.2%), 527 (0.2%), 606 (0.23%), 633 (M^+ + 1, 0.2%); ^{1}H NMR (DMSO-d_6) δ 1.40 (s, 4H, CH_2CH$_2$N), 3.13 (m, 4H, 2CH$_2$N), 4.37 (s, 4H, 2CH$_2$S), 4.65 (s, 4H, 2CH$_2$O), 7.08–7.12 (m, 4H, ArH's), 7.51–7.58 (m, 4H, ArH's), 8.01 (t, 2H, J = 5.4 Hz, 2NH), 9.14 (s, 2H, triazole-3H) ppm; ^{13}C NMR (DMSO-d_6) δ 26.37, 26.53, 38.13, 67.46 (aliphatic C's), 113.18, 120.90, 121.56, 124.07, 130.07, 132.95, 143.11, 156.34, 157.12, 167.13 (CO) ppm. Anal. calcd for $C_{28}H_{28}N_{10}O_4S_2$ (632.72): C, 53.15; H, 4.46; N, 22.14%. Found: C, 53.27; H, 4.54; N, 22.24%.

4.1.5. Synthesis of bis((quinoxalin-2-yl)phenoxy)alkane derivatives 10a–e

4.1.5.1 General procedure. To a mixture of the appropriate bis(α-bromoacetophenone) derivative **6a**, **b**, **d** and *o*-phenylenediamine derivatives **9a**, **b** (2 mmol) in ethanol (25 mL), piperidine (0.19 mL, 2 mmol) was added. The reaction mixture was heated under reflux for 3 h. The solvent was then removed under *vacuum*, and the solid product was collected by filtration, dried and recrystallized from ethanol to afford the corresponding bis-quinoxaline derivatives **10a–e**.

*4.1.5.2 N,N′-(Ethane-1,2-diyl)bis(2-(4-(quinoxalin-2-yl) phenoxy)acetamide) (**10a**).* From **6a** and **9a**, crystalized from dioxane as yellow crystals, yield 55%, mp 250–252 °C; IR (KBr) ν 3433 (NH), 1643 (C=O), 1620 (C=N) cm^{-1}; MS *m*/*z* (%): 102 (77%), 235 (100%), 293 (54%), 350 (17%), 526 (8%), 584 (M^+, 38%); ^{1}H NMR (DMSO-d_6) δ 3.30 (m, 4H, 2CH$_2$N), 4.58 (s, 4H, 2CH$_2$O), 7.15 (d, 4H, J = 8.7 Hz, ArH's), 7.73–7.84 (m, 4H, ArH's), 8.04 (d, 4H, J = 8.7 Hz, ArH's), 8.24–8.27 (m, 6H, 4ArH's & 2NH), 9.47 (s, 2H, quinoxaline-3-H) ppm; ^{13}C NMR (CDCl$_3$, APT) δ 39.13, 67.49 (2CH$_2$), 126.37, 140.84, 141.78, 151.47, 154.92, 168.81 (6C's), 112.85, 122.59, 128.88, 129.82, 130.43, 131.62, 146.13 (7CH's) ppm. Anal. calcd for $C_{34}H_{28}N_6O_4$ (584.64): C, 69.85; H, 4.83; N, 14.38%. Found: C, 69.74; H, 4.95; N, 14.26%.

*4.1.5.3 N,N′-(Ethane-1,2-diyl)bis(2-(4-(6,7-dimethylquinoxalin-2-yl)phenoxy)acetamide) (**10b**).* From **6a** and **9b**, crystalized from DMF as yellow crystals, yield 60%, mp 254–256 °C IR (KBr) ν 3356 (NH), 1643 (C=O), 1620 (C=N) cm^{-1}; MS *m*/*z* (%): 103 (57%), 233 (58%), 250 (100%), 263 (89%), 320 (39%), 378 (17%), 515 (4%), 612 (3%), 640 (M^+, 89%); ^{1}H NMR (DMSO-d_6) δ 2.42 (s, 12H, 4CH$_3$), 3.33 (m, 4H, 2CH$_2$N), 4.55 (s, 4H, 2CH$_2$O), 7.09 (d, 4H, J = 8.7 Hz, ArH's), 7.77 (s, 4H, 2ArH's & 2NH), 8.16 (m, 6H, ArH's), 9.29 (s, 2H, quinoxaline-3H) ppm. Anal. calcd for $C_{38}H_{36}N_6O_4$ (640.74): C, 71.23; H, 5.66; N, 13.12%. Found: C, 71.12; H, 5.70; N, 13.01%.

*4.1.5.4 N,N′-(Ethane-1,2-diyl)bis(2-(2-(quinoxalin-2-yl) phenoxy)acetamide) (**10c**).* From **6d** and **9a**, crystalized from ethanol as brown crystals, yield 50%, mp 210–212 °C; IR (KBr) ν 3341 (NH), 1666 (C=O), 1600 (C=N) cm^{-1}; MS *m*/*z* (%): 102 (24%), 207 (21%), 235 (100%), 292 (24%), 349 (9%), 554 (10%), 584 (M^+, 43%); ^{1}H NMR (CDCl$_3$) δ 3.43 (m, 4H, 2CH$_2$N), 4.46 (s, 4H, 2CH$_2$O), 6.94 (d, 2H, J = 8.1 Hz, ArH's), 7.17 (t, 2H, J = 7.5 Hz, ArH's), 7.44 (t, 2H, J = 6.9 Hz, ArH's), 7.68–7.76 (m, 8H, 6ArH's & 2NH), 7.99–8.02 (m, 4H, ArH's), 9.07 (s, 2H, quinoxaline-3H) ppm. Anal. calcd for $C_{34}H_{28}N_6O_4$ (584.64): C, 69.85; H, 4.83; N, 14.38%. Found: C, 69.77; H, 4.77; N, 14.25%.

*4.1.5.5 N,N′-(Propane-1,3-diyl)bis(2-(4-(quinoxalin-2-yl) phenoxy)acetamide) (**10d**).* From **6a** and **9a**, crystalized from ethanol as brown crystals, yield 66%, mp 184–186 °C; IR (KBr) ν 3418 (NH), 1659 (C=O), 1610 (C=N) cm^{-1}; MS *m*/*z* (%): 98 (69%), 121 (19%), 205 (6%), 235 (100%), 281 (14%), 364 (30%), 512 (5%), 598 (M^+, 17%); ^{1}H NMR (DMSO-d_6) δ 1.65 (quintet, 2H, J = 6.6 Hz, CH$_2$CH_2CH$_2$), 3.10–3.25 (m, 4H, 2CH$_2$N), 4.61 (s, 4H, 2CH$_2$O), 7.17 (d, 4H, J = 8.1 Hz, ArH's), 7.80 (m, 4H, ArH's), 8.06 (d, 4H, J = 7.8 Hz, ArH's), 8.21 (brs, 2H, 2NH), 8.30 (d, 4H, J = 8.4 Hz, ArH's), 9.50 (s, 2H, quinoxaline-3H) ppm. Anal. calcd for $C_{35}H_{30}N_6O_4$ (598.66): C, 70.22; H, 5.05; N, 14.04%. Found: C, 70.29; H, 4.94; N, 13.89%.

*4.1.5.6 N,N′-(Butane-1,4-diyl)bis(2-(2-(6,7-dimethylquinoxalin-2-yl)phenoxy)acetamide) (**10e**).* From **6f** and **9b**, crystalized from DMF/ethanol as yellow crystals, yield 70%, mp 210–212 °C; IR (KBr) ν 3240 (NH), 1674 (C=O), 1620 (C=N) cm^{-1}; MS *m*/*z* (%): 103 (17%), 235 (21%), 249 (19%), 263 (100%), 405 (6%), 638 (3%), 668 (M^+, 32%); ^{1}H NMR (CDCl$_3$) δ 1.29 (s, 4H, 2 CH_2CH$_2$N), 2.46 (s, 12H, 4CH$_3$), 3.19–3.21 (m, 4H, 2 NHCH_2CH$_2$), 4.59 (s, 4H, 2CH$_2$O), 7.02 (d, 2H, J = 8.1 Hz, ArH's), 7.17 (t, 2H, J = 7.5 Hz, ArH's), 7.35 (s, 2H, 2NH), 7.43 (t, 2H, J = 7.5 Hz, ArH's), 7.65–7.75 (m, 6H, ArH's), 8.93 (s, 2H, quinoxaline-3H) ppm; ^{13}C NMR (CDCl$_3$, APT) δ 20.35, 20.41 (2CH$_3$), 26.45, 38.35, 67.61 (3CH$_2$'s, aliphatic), 112.79, 122.52, 127.73, 127.78, 131.38, 131.54, 144.83 (7CH's), 126.48, 139.74, 140.46, 140.69, 141.10, 150.27, 154.85, 167.91 (8C's) ppm. Anal. calcd for $C_{40}H_{40}N_6O_4$ (668.80): C, 71.84; H, 6.03; N, 12.57%. Found: C, 71.79; H, 6.22; N, 12.45%.

4.2. Biological assays

The biological activity of the synthesized molecules including cytotoxicity against breast cancer cell lines (MDA-MB-231 cells), enzymes' assay of the most active compounds, Annexin V-FITC/Propidium iodide dual staining assay for measuring the apoptotic effect of compound **8i** were done at Center of Excellence in tissue culture in the National research institute and Suez Canal University, Egypt.

4.3. Cytotoxicity

Breast cancer cell lines (MCF-7 and MDA-MB-231), and the normal breast cell lines (MCF-10A) were collected from National Cancer Institute in Cairo and grown in "RPMI-1640 medium L-glutamine. The cells were grown in 10% fetal bovine serum (FBS) and 1% penicillin-streptomycin. All samples were cultured at 37 degrees Celsius in a 5% CO_2 gas. On the second

day, the cells were grown in triplicate on a 96-well plate at a density of 5×10^4 cells and incubated with the investigated compounds at concentrations; 0.01, 0.1, 1, 10, and 100 μM. MTT solution was used to determine the cell viability. The plate was cultured for 3 hours. An ELISA microplate reader was used to measure the absorbance. The viability was determined by comparing it to the control group, and the IC_{50} values were recorded.[58,59]

4.4. Enzymatic targeting

To assess the inhibitory potency of compound **8i** against the PARP-1 and EGFR target proteins. Research kits of PARP-1 (Bioscience, Cat no. # 80580, CA, USA) and EGFR (ADP-GloTM kinase assay, Cat no. V9261, Promega, USA), were employed. The percentage inhibition of autophosphorylation by substances was estimated using the following equation: $\text{percentage inhibition} = 100 - \left[\frac{\text{control}}{\text{treated}} - \text{control}\right]$.[60,61]

4.5. Apoptosis investigation

MDA-MB-231 cells were incubated overnight in 6-well culture plates ($3–5 \times 10^5$ cells per well) and then treated with the IC_{50} values of compound **8i** for 48 hours. After that, the cells were incubated in a 100 μL solution of Annexin binding buffer "25 mM $CaCl_2$, 1.4 M NaCl, and 0.1 M Hepes/NaOH at pH 7.4" in the dark for 30 minutes with "Annexin V-FITC solution (1 : 100) and propidium iodide (PI) at a concentration equivalent to 10 μg mL^{-1}". The labeled cells were then extracted using the Cytoflex FACS machine. CytExpert software was used to analyze the data.[62,63]

4.6. Molecular docking studies

Molecular modeling studies were carried out using Chimera-UCSF and AutoDock Vina on Linux-based systems at the laboratory of Drug Design and Discovery, Suez Canal University. Proteins and compounds structures were prepared and optimized using Maestro, then binding sites inside proteins were determined using grid-box dimensions around the co-crystallized ligands. The investigated compounds were docked against the protein structures of PARP-1 (PDB = 5DS3) EGFR (PDB = 1XKK) using AutoDock Vina software following routine work.[64] Vina was used to improve protein and ligand structures and to favor them energetically. Binding activities interpreted molecular docking results in terms of binding energy and ligand–receptor interactions. The visualization was then done with Chimera.

Conflicts of interest

The authors declare that there is no conflict-of-interest text.

References

1 H. Sung, J. Ferlay, R. L. Siegel, M. Laversanne, I. Soerjomataram, A. Jemal and F. Bray, *Ca-Cancer J. Clin.*, 2021, **71**, 209.
2 P. A. Jeggo and M. Löbrich, *Biochem. J.*, 2015, **471**, 1.
3 S. Kumari, A. V. Carmona, A. K. Tiwari and P. C. Trippier, *J. Med. Chem.*, 2020, **63**, 12290.
4 R. M. de Figueiredo, J. S. Suppo and J. M. Campagne, *Chem. Rev.*, 2016, **116**, 12029.
5 V. R. Pattabiraman and J. W. Bode, *Nature*, 2011, **480**, 471.
6 A. Johansson, P. Kollman, S. Rothenberg and J. McKelvey, *J. Am. Chem. Soc.*, 1974, **96**, 3794.
7 W. Sneader, in *Comprehensive Medicinal Chemistry*, ed. C. Hansch, P. G. Sammnes and J. B. Taylor, Pergamon, London, 1990, vol. 1, p. 65.
8 R. Aggarwal and G. Sumran, *Eur. J. Med. Chem.*, 2020, **205**, 112652.
9 X. Jiang, K. Wu, R. Bai, P. Zhang and Y. Zhang, *Eur. J. Med. Chem.*, 2022, **229**, 114085.
10 N. A. Alsaif, M. A. Dahab, M. M. Alanazi, A. J. Obaidullah, A. A. Al-Mehizia, M. M. Alanazi, S. Aldawas, H. A. Mahdy and H. Elkady, *Bioorg. Chem.*, 2021, **110**, 104807.
11 L. Fabian, M. Taverna Porro, N. Gomez, M. Salvatori, G. Turk, D. Estrin and A. Moglioni, *Eur. J. Med. Chem.*, 2020, **188**, 111987.
12 X. Lu, H. Chen, A. V. Patterson, J. B. Smaill and K. Ding, *J. Med. Chem.*, 2019, **62**, 2905.
13 S. Dai, Z. Zhou, Z. Chen, G. Xu and Y. Chen, *Cells*, 2019, **8**, 614.
14 M. S. Ayoup, M. A. Fouad, H. Abdel-Hamid, E.-S. Ramadan, M. M. Abu-Serie, A. Noby and M. Teleb, *Eur. J. Med. Chem.*, 2020, **186**, 111875.
15 M. P. Gajewski, H. Beall, M. Schnieder, S. M. Stranahan, M. D. Mosher, K. C. Rider and N. R. Natale, *Bioorg. Med. Chem. Lett.*, 2009, **19**, 4067.
16 M. I. El-Gamal, M. S. Abdel-Maksoud, M. M. G. El-Din, K. H. Yoo, D. Baek and C. H. Oh, *Arch. Pharm.*, 2014, **347**, 635.
17 I. Khan, A. Ibrar and N. Abbas, *Eur. J. Med. Chem.*, 2013, **63**, 854.
18 A.-M. M. E. Omar, O. M. AboulWafa, M. E. Amr and M. S. El-Shoukrofy, *Bioorg. Chem.*, 2021, **109**, 104752.
19 W. Ma, P. Chen, X. Huo, Y. Ma, Y. Li, P. Diao, F. Yang, S. Zheng, M. Hu, W. You and P. Zhao, *Eur. J. Med. Chem.*, 2020, **208**, 112847.
20 Z. Liu, B. Lang, M. Gao, X. Chang, Q. Guan, Q. Xu, D. Wu, Z. Li, D. Zuo, W. Zhang and Y. Wu, *J. Cell. Biochem.*, 2020, **121**, 2184.
21 A. U. Çevik, B. N. Sağlık, D. Osmaniye, S. Levent, B. K. Çavuşoğlu, A. B. Karaduman, Y. Özkay and Z. A. Kaplancıklı, *Arch. Pharm.*, 2020, **353**, e2000008.
22 F. Yang, X.-E. Jian, L. Chen, Y.-F. Ma, Y.-X. Liu, W.-W. You and P.-L. Zhao, *New J. Chem.*, 2021, **45**, 21869.
23 I. Khan, S. Zaib, A. Ibrar, N. H. Rama, J. Simpson and J. Iqbal, *Eur. J. Med. Chem.*, 2014, **78**, 167.
24 I. Khan, A. Ibrar, S. Zaib, S. Ahmad, N. Furtmann, S. Hameed, J. Simpson, J. Bajorath and J. Iqbal, *Bioorg. Med. Chem.*, 2014, **22**, 6163.
25 H. A. M. El-Sherief, B. G. M. Youssif, S. N. A. Bukhari, A. H. Abdelazeem, M. Abdel-Aziz and H. M. Abdel-Rahman, *Eur. J. Med. Chem.*, 2018, **156**, 774.

26 A. T. A. Boraei, P. K. Singh, M. Sechi and S. Satta, *Eur. J. Med. Chem.*, 2019, **182**, 111621.
27 A. T. A. Boraei, H. A. Ghabbour, M. S. Gomaa, E. S. H. El Ashry and A. Barakat, *Molecules*, 2019, **24**, 4471.
28 R. Aggarwal, M. Hooda, P. Kumar and G. Sumran, *Top. Curr. Chem.*, 2022, **380**, 10.
29 M. Kumar, G. Joshi, S. Arora, T. Singh, S. Biswas, N. Sharma, Z. R. Bhat, K. Tikoo, S. Singh and R. Kumar, *Molecules*, 2021, **26**, 1490.
30 A. Iwashita, K. Hattori, H. Yamamoto, J. Ishida, Y. Kido, K. Kamijo, K. Murano, H. Miyake, T. Kinoshita, M. Warizaya, M. Ohkubo, N. Matsuoka and S. Mutoh, *FEBS Lett.*, 2005, **579**, 1389–1393.
31 G. Papeo, P. Orsini, N. R. Avanzi, D. Borghi, E. Casale, M. Ciomei, A. Cirla, V. Desperati, D. Donati, E. R. Felder, A. Galvani, M. Guanci, A. Isacchi, H. Posteri, S. Rainoldi, F. Riccardi-Sirtori, A. Scolaro and A. Montagnoli, *ACS Med. Chem. Lett.*, 2019, **10**, 534.
32 Y.-H. Kang, M.-J. Yi, M.-J. Kim, M.-T. Park, S. Bae, C.-M. Kang, C.-K. Cho, I.-C. Park, M.-J. Park, C. H. Rhee, S.-I. Hong, H. Y. Chung, Y.-S. Lee and S.-J. Lee, *Cancer Res.*, 2004, **64**, 8960.
33 P. Wee and Z. Wang, *Cancers*, 2017, **9**, 52.
34 M. M. Alam, *Arch. Pharm.*, 2022, **355**, 2100158.
35 A. C. Pinheiro, T. C. M. Nogueira and M. V. N. de Souza, *Anti-Cancer Agents Med. Chem.*, 2016, **16**, 1339.
36 A. Powelczyk, K. S. Kasprzak, D. Olender and L. Zaprutko, *Int. J. Bio. Sci.*, 2018, **19**, 1104.
37 N. Keru, P. Singh, N. Koorbanally, R. Raj and V. Kumar, *Eur. J. Med. Chem.*, 2017, **142**, 179.
38 K. Nepali, S. Sharma, M. Sharma, P. M. S. Bedi and K. L. Dhar, *Eur. J. Med. Chem.*, 2014, **77**, 422.
39 R. Dent, M. Trudeau, K. I. Pritchard, W. M. Hanna, H. K. Kahn, C. A. Sawka, L. A. Lickley, E. Rawlinson, P. Sun and S. A. Narod, *Clin. Cancer Res.*, 2007, **13**, 4429–4434.
40 E. K. Lee and U. A. Matulonis, *Cancers*, 2020, **12**, 2054.
41 S. Lin, X. Zhang, Z. Yu, X. Huang, J. Xu, Y. Liu and L. Wu, *Bioorg. Med. Chem.*, 2022, **61**, 116739.
42 W. K. A. Yung, S. Wu, F. Gao, S. Zheng, J. Ding, C. Zhang, X. Li, R. Ezhilarasan, N. Feng, J. F. De Groot, E. P. Sulman, T. Heffernan and D. Koul, *J. Clin. Oncol.*, 2019, **37**, 2047.
43 J.-M. Contreras and J.-J. Bourguignon, in *The Practice of Medicinal Chemistry*, ed. C. G. Wermuth, Academic Press, London, 2nd edn, 2003, pp. 251–273.
44 M. J. Wasko, K. A. Pellegrene, J. D. Madura and C. K. Surratt, *Front. Neurol.*, 2015, **6**, 197.
45 A. A. Abbas, M. H. Abdellattif and K. M. Dawood, *Expert Opin. Ther. Pat.*, 2022, **32**, 63.
46 K. M. Dawood, M. A. Raslan, A. A. Abbas, B. E. Mohamed and M. S. Nafie, *Anti-Cancer Agents Med. Chem.*, 2022, DOI: **10.2174/1871520622666220615140239**.
47 K. M. Dawood and A. A. Abbas, *ChemistrySelect*, 2021, **6**, 279–305.
48 K. M. Dawood, M. A. Raslan, A. A. Abbas, B. E. Mohamed, M. H. Abdellattif, M. S. Nafie and M. K. Hassan, *Front Org. Chem.*, 2021, **9**, 694870.
49 K. M. Dawood and A. A. Abbas, *Expert Opin. Ther. Pat.*, 2020, **30**, 695–714.
50 K. M. Dawood and H. K. A. Abu-Deif, *Chem. Pharm. Bull.*, 2014, **62**, 439.
51 B. Hegazi, H. A. Mohamed, K. M. Dawood and F. A. R. Badria, *Chem. Pharm. Bull.*, 2010, **58**, 479.
52 K. M. Dawood, *J. Heterocycl. Chem.*, 2019, **56**, 1701.
53 K. M. Dawood, A. M. Farag and H. A. Abdel-Aziz, *Heteroatom Chem*, 2005, **16**, 621.
54 H. Abdel-Gawad, H. A. Mohamed, K. M. Dawood and F. A. R. Badria, *Chem. Pharm. Bull.*, 2010, **58**, 1529.
55 H. K. Mahmoud, A. A. Abbas and S. M. Gomha, *Polycycl. Aromat. Compd.*, 2021, **41**, 2029.
56 R. M. Kassab, F. S. Khalil and A. A. Abbas, *Polycycl. Aromat. Compd.*, 2022, **42**(5), 2751–2766.
57 M. S. Nafie, S. M. Kishk, S. Mahgoub and A. M. Amer, *Chem. Biol. Drug Des.*, 2022, **99**, 547.
58 T. Mosmann, *J. Immunol. Methods*, 1983, **65**, 55.
59 M. S. Nafie, N. H. Elghazawy, S. M. Owf, K. Arafa, M. A. Abdel-Rahman and R. K. Arafa, *Chem.-Biol. Interact.*, 2022, **351**, 109753.
60 H. S. A. ElZahabi, M. S. Nafie, D. Osman, N. H. Elghazawy, D. H. Soliman, A. A. H. EL-Helby and R. K. Arafa, *Eur. J. Med. Chem.*, 2021, **222**, 113609.
61 S. K. Ramadan, E. Z. Elrazaz, K. A. M. Abouzid and A. M. El-Naggar, *RSC Adv.*, 2020, **10**, 29475.
62 M. S. Nafie, A. M. Amer, A. K. Mohamed and E. S. Tantawy, *Bioorg. Med. Chem.*, 2020, **28**, 115828.
63 M. S. Nafie and A. T. A. Boraei, *Bioorg. Chem.*, 2022, **122**, 105708.
64 M. S. Nafie, M. A. Tantawy and G. A. Elmgeed, *Steroids*, 2019, **152**, 108485.